EVALUATION AND IMPLEMENTATION OF ROCK INDENTATION TESTS EXPERIMENTALLY AND NUMERICALLY ON HIGH STRENGTH AND ISOTROPIC ROCKS

By

Prajit Premraj

A thesis submitted to the School of Graduate Studies in partial fulfillment of the requirements for the degree of

Master of Engineering

Faculty of Engineering and Applied Science Memorial University of Newfoundland

May 2023

St. John's, Newfoundland and Labrador, Canada

Abstract

A comprehensive study of rock indentation was performed at Memorial University of Newfoundland (MUN). Testing was performed on hard rocks such as granite as well as medium-strength rocks such as rock like material (RLM) which were manufactured in the Drilling Laboratory of MUN by researchers. For the two types of testing procedures utilized, samples were prepared accordingly. Metallic indenters were then forced against the rock core specimens under controlled loading conditions. Graphical analysis of the loading cycles were then analyzed and studied. As there was no fixed industrial standard, a procedure was devised and deployed for the indentation test of rock. Empirical correlations from work done by researchers in the past were adjusted with modifications from the indentation tests and augmented to predict the strength of the rocks. With the help of the PFC 2D software package, the experiment was replicated numerically. In conclusion, the slope of the loading curves from the experiment and numeric modeling was used to predict the strength of the rock.

A very detailed study was conducted on the variables affecting the indentation tests in which the effect of individual variables such as confinement, size of the specimen, and geometry of the testing metallic indenter were investigated. The study was concluded by reaching and recording the failure point and the specific energy utilized in the rock breakage.

Acknowledgements

They are right when they say time flies when you are busy doing something you love. The two-year journey of research and academics that made up my Master's program has given me a lot to learn academically and practically, effectively shaping me into a professional in the industry I strive to work for. There have been times I felt lost, but with the help of the people I was surrounded by, I was able to reach this pinnacle of achievement. From completing academic courses to suggesting research options, the road from student to researcher has been very fascinating, and this goal would have remained a dream without the recourses of the members of the Drilling Technology Laboratory (DTL).

I would like to express my sincere gratitude to the Memorial University of Newfoundland for allowing me to accomplish my dream of studying in an institution with amenities of such high standards that have augmented my research work in the best way possible.

I would like to deeply thank my supervisor, Dr. Stephen Butt, for having showered me with his diverse knowledge and directed me on the right path using his extensive experience and teachings. It was an honor for me to learn and work under his supervision.

I would also like to thank our lab manager, Dr. Abdelsalam Abugharara, for assisting me with my work in the laboratory, and my colleague Zijian Li for offering endless support throughout my term. I am also grateful to Steve Steele for his technical help with my experiments and Technical Services at Memorial University in helping manufacture my experimental apparatus. Last but certainly not the least, this journey would have been impossible without my family's encouragement, prayers and love.

Table of Contents

List of Figures

List of Tables

List of Symbols and Abbreviations

ISRM	International Society for Rock Mechanics
ASTM	American Society for Testing Materials
ASME	American Society of Mechanical Engineers
CGS	Canadian Geotechnical Society
OMAE	Offshore Mechanics and Arctic Engineering
UCS	Unconfined Compressive Strength
HRC	Rockwell Hardness on C- Scale
PLI	Point Load Index
ITS	Indirect Tensile Strength
BTS	Brazilian Tensile Strength
IHI	Indentation Hardness Index
DEM	Distinct Element Model
FEM	Finite Element Model
ROP	Rate of Penetration
WOB	Weight on bit
MS RLM	Medium strength rock like material
μ	Poisson's ratio
R^2	Coefficient of Determination
α	Apex Angle
E	Young's Modulus
P-wave	Primary wave
S-wave	Secondary wave

TBM	Tunnel Boring Machine
PFC2D	Particle flow code in two dimensions
IT Coefficient	Indentation Test Coefficient
SE	Specific Energy
L: D	Length to diameter ratio
MUN	Memorial University of Newfoundland

Chapter 1: Introduction

1.1 Background

The subsurface of the Earth's surface has many natural resources of great economic value. These resources range from minerals and metal ores to petroleum, but the excavation and drilling processes required to recover these resources are very expensive and difficult tasks. To tackle this challenge, we can utilize the ability to predict the time needed to drill a certain type of rock which helps us to set economic boundaries. This requires the engineers to know the strength of rocks. Ideally, we would use the direct measurements for the strength, but these are less suited to field conditions, expensive, and time consuming. Having an indirect measurement of the strength of these rocks is therefore a great solution. Indentation of rock, which is an indicator of material hardness, is one such technique. This involves forcing a conical metal indenter against a rock volume perpendicular to the surface until a crater forms. The graphical analysis of this experimental method helps us to better understand the rock breakage happening beneath the indenter. The principle of rock excavation in mining and oil and gas drilling is primarily breaking the rock by indenting into it. The indentation test has been performed on rocks for decades by various researchers and has undergone many modifications. There is no standardized procedure for performing the test, but an ISRM draft provide insight into how to perform the test.

1.2 Research Motivation and objectives

All mining processes imply excavation of the earth's crust to extract the valuable ore buried beneath its subsequent layers. The efficiency of the mining tools used in these processes

relies on the technology deployed for the extraction of ore. Furthermore, the tools responses vary with respect to different rock types ranging from low strength to high strength. These rock mechanical parameters, such as UCS, have a significant impact on the design of rock engineering projects (Santarelli, 1996). We can determine the UCS one of two ways; use standard laboratory tests defined by ASTM (1984) and ISRM (1979), or utilize logging of wells. Swain (1976) stated that, because rocks are complicated formations with opaque surfaces, any testing done on them is limited to before and after external visualization tests. For a core sample to yield accurate data for UCS measurements, the rock must have no weak points in its strength, no discontinuities, and no micro-cracks. However, due to the high cost of cored samples and their scarcity, unconventional procedures are sometimes used (Theircelin and Cook, 1988). USC testing is also problematic due to high costs, time restrictions, and the difficulties of obtaining undamaged core samples. Conclusively, direct strength tests are more complicated, expensive, more time-consuming, and less adaptable to field conditions in comparison to indirect or unconventional tests (Raj, 2015). Indentation tests are an indirect way of finding the rock's strength. On the other hand, indentation is the mechanism by which the drilling tools break the rock by applying a force normal to its surface. According to T.Szwedziki's earlier research and experiments, an indentation hardness test is an indirect approach that may be used to correlate with unconfined compressive strength since they have a linear connection for particular rock types (1998). ISRM proposed a standard IHI test that predicted UCS from indentation testing. The work was standardized but then taken down after which the testing procedure underwent a lot of modification and improvements for two decades (Yagiz, 2012). Not only does the indentation testing help us in predicting

strength, but it also indicates the drillability of the rock sample which allows us to augment the efficiency of the design of mining tools and equipment we choose to use. In addition to this, it is important to note that most of the rock-cutting tools that we have are indenters. This makes it more important to investigate the deformation and the mechanism in which the rock breaks under indentation (Artsimovic, 1978).

On a smaller scale, to learn and analyze the indentation process well, a rock mass is normally subjected to loading using a small indenter under controlled systems of displacement or load (Kalyan, 2015). Unlike direct strength tests, these tests do not require as sophisticated a sample preparation (T.Szwedziki, 1998). The variables tested, such as the indenter geometry, the loading rate, sample dimensions, confinement around the sample, etc., lead to different responses. The study about crater formation, initiated by Maurer (1960), describes indentation as a 3-stage process, beginning where the indenter crushes the rock surface causing elastic deformation, an extension of the cracks, and ending with chip formation. The middle stage carries a lot of value to the engineers as the slope of the indentation curve helps us understand the behavior of crushing.

With varying testing procedures introduced by several researchers, this work aims to standardize a procedure for the test. The work also focuses on replicating the experimental work numerically and validating the results using a distinct element-modeling package called the PFC2D. With these tests, the strength of the rocks is predicted using correlations from research conducted in past. In addition, part of the work was dedicated to responding to rock breakage in indentation concerning different variables in the test. The different variables utilized for the study are sample sizes, confinement and tip diameter of the metallic indenter. Studying these changing patterns in these tests would help us to

understand the conditions in which rocks break easily and with minimum energy utilization. Therefore a methodology to predict the specific energy from indentation test was proposed. Based on this, the tools for efficient excavation can be designed.

The long term goal of this study is to predict the rate of penetration on rock types from indentation tests performed in the laboratory.

1.3 Thesis Outline:

This thesis consists of 5 chapters. **Chapter 1** deals with discussing the background of the SMD project work and how the mechanism of fragmentation leads us to different goals to be achieved in the long term. It elaborates on the motivations and objectives of the research and delineates the contents of this thesis. This thesis is based on two conference papers, one of the two publications that was accepted for the OMAE 2022, and the other which has been accepted by GeoCalgary 2022.

Chapter 2 is a very comprehensive literature review about the indentation of rocks. It includes the principles and mechanism of the indentation on rocks, the rocks indexes, their correlations, and most importantly, the studies conducted on all the variables involved in and affecting the process. These experimental process and studies are also augmented with Distinct Element Modelling (DEM) used to simulate the experimental work numerically.

Chapter 3 deals with the experimental methodology for the indentation tests in depth. It covers aspects such as materials used and their characterization, the apparatus used in the experimental tests, sample preparation for the tests, and a detailed stepwise procedure to perform the tests to produce efficient and repeatable results. The efficiency and repeatability of the test results were by cause of a very strict sample preparation procedure

and proper calibration of the servo control. The chapter enumerates a detailed, step-wise procedure for performing the tests, estimating a very small crater volume, and determining the Specific Energy spent in cratering into the rock. It also helps the reader by gathering information needed for understanding the research in Chapters 4 and 5 effectively.

Chapter 4 is the Indentation test implementation for rock strength correlation by Experimental method and simulation using the Distinct element method, which concludes with an agreement in the indentation test from the laboratory and simulation work. The result from the study was correlated to rock strength using previous research work with slight modifications in the empirical equations proposed by researchers in the past. The work also suggests a procedure to perform the test with reduced exertion in precise sample preparations to predict the rock strength with less expenditure.

Chapter 5 deals with the evaluation of indentation on high strength and isotropic formations. The study takes into account the application of metallic indenters with varying tip diameters on high strength rock cores of varying sizes under confined and unconfined conditions. In addition, the results of these tests are linked with a specific energy study. The study concludes with conditions in which the rock can be fragmented most efficiently.

Chapter 6 presents the conclusion and recommendation underlining the main findings and a summary along with references for future work in this disc cutter penetration study.

Chapter 2: Literature Review

2.1 Overview of Indentation Test

As a general explanation, oil and gas drilling and mining processes aim to recover natural resources from the subsurface of the Earth. The successful recovery of these valuable resources is achieved by excavation and drilling processes. The accomplishment of such projects depends on how efficiently drilling and excavation are performed, but these processes are time-consuming and expensive. Achieving efficiency in these processes requires knowledge of the rock properties to be drilled and choosing the right tools for excavation. The mechanism by which the rocks are crushed and cratered with the tools forced into the rock is called rock indentation.

Rock indentation is one of the indirect rock testing methods that help identify the hardness of the rocks. With known empirical correlations, these tests are a tool for predicting the strength of rocks in field conditions with high confidence. (Szwedzicki, 1998), (Leite, 2000), (Copur, 2003). In addition to this, most of the tools used for drilling have teeth on the drilling bits or sharp edges on discs, and so the indentation test was also meant to have the potential in predicting the rate of penetration while drilling with a bit that had teeth acting like indenters used in the test. With the slope of the plot of indentation of rocks, a drilling rate prediction model was generated. (Morris, 1969), (Kahraman, 2000).

Due to its opaque nature, the effectiveness of the test could only be determined through visualization of the rock before and after conducting the destructive test (Swain, 1976). The use of an electron microscope aided in viewing the cracks of the rocks and their

transition (Thiercelin & Cook, 1988). More research was targeted in categorizing the types of cracks underneath the indenter and identifying inter grain tensile cracks as the most dominant crack type. (Zhu, 2020).

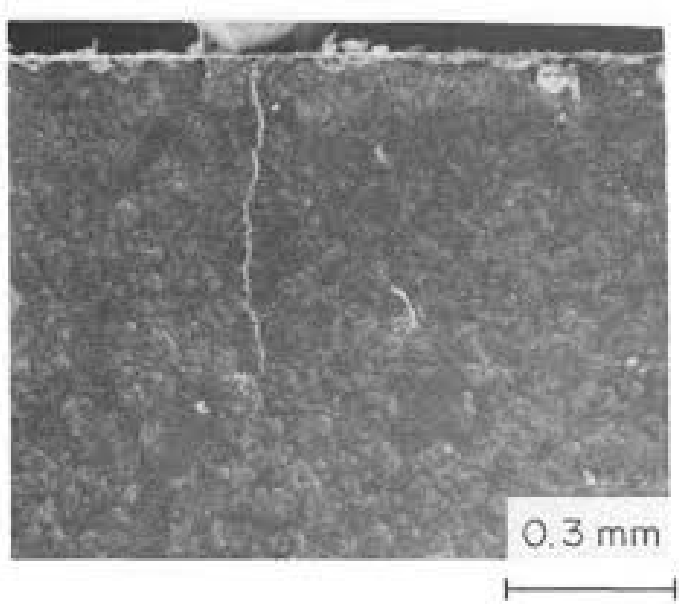

Figure 2-1: Crack initiation under an electron microscope on a limestone sample. (Lindqvist, 1984)

As seen in Figure 2-1, a continuous vertical crack can be seen penetrating downwards, originating from beneath the tip diameter.

Many different researchers carried out indentation on all three types of rocks occurring in nature – igneous, metamorphic, and sedimentary – by using a controlled loading procedure and then presented their findings. (Hood,1977),(Cook,1984), (Lindquist,1984). Notably, the absence of a standardized draft for the indentation testing has resulted in many modifications over several decades. When a metallic indenter is forced normally against the surface of the rock, a series of rock breakage patterns are observed beneath the indenter.

The rock is crushed, followed by fracturing, and ending with the chipping of the rock. Several researchers have conducted indentation on different types of rocks along with varying indenter shapes, loading rates of compression, confinements around the rock specimens, and the size of the rock samples. (Lindquist,1982), (Cook,1984), (Pang,1990), (Premraj, 2022).

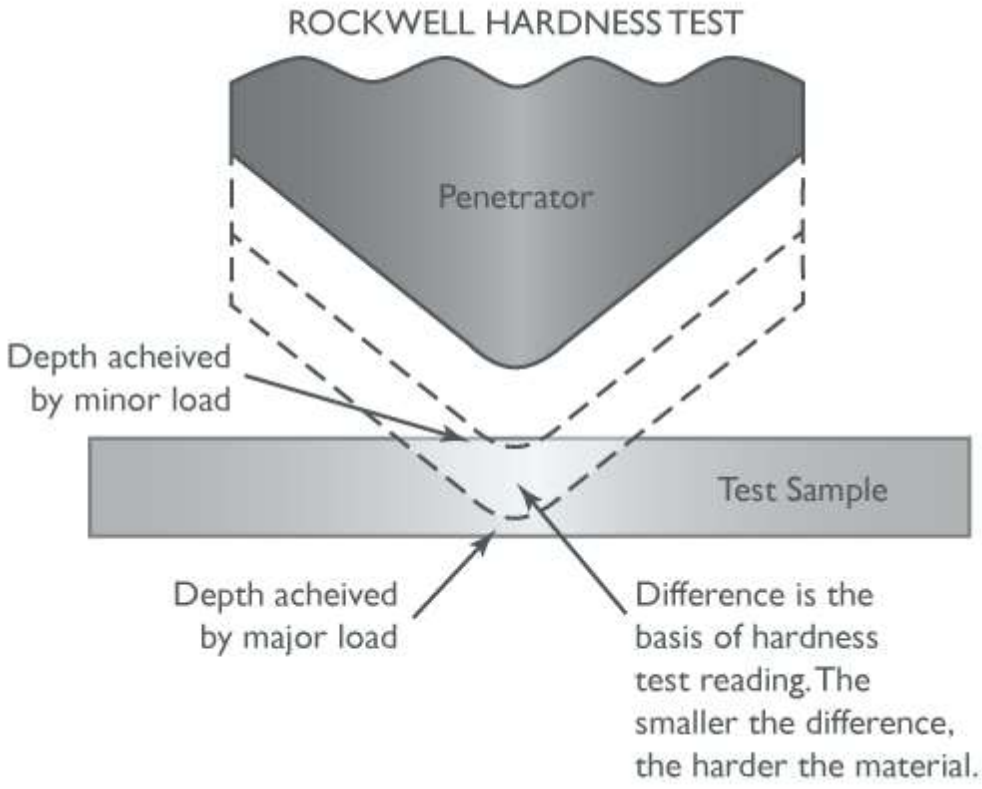

Figure 2-2: Indentation testing on metals for hardness. (Liggett, 2000)

The hardness testing method was initially developed for metals where the indentation of the conical pick determined the hardness of the metal; Figure 2-2 above illustrates how the testing was executed. Metals have a ductile nature, and when loading occurs, there is anelastic deformation region before the plastic deformation occurs. Rocks, on the other hand, possess an elastic nature at the beginning of the loading cycle and transition into

plastic deformation. (Hood, 1977).

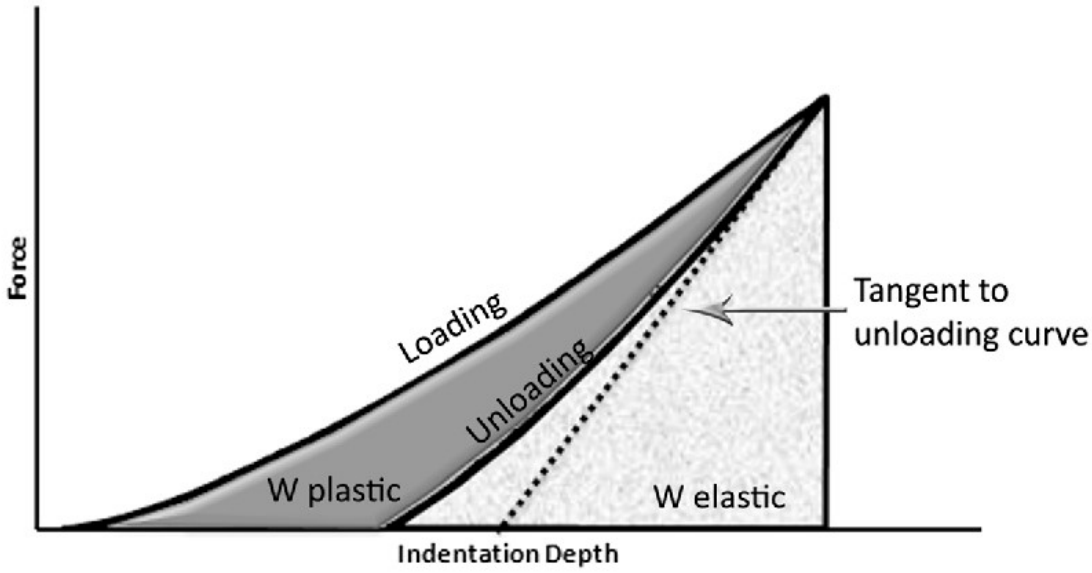

Figure 2-3: Graphical response of the indentation test on rocks. (Zinelis, 2015)

From Figure 2-3, a graphical study of the loading curve helps us learn more about the rock properties. With increasing loads, the tip of the indenter penetrates deeper into the rock. The dark grey area under the curve between the loading and unloading cycle is equivalent to the work done for cratering the rock. This is used for the specific energy study while characterizing excavation tool performance (Kalyan, 2016). According to Teale's work on developing an expression to calculate the specific energy from drilling operations, the expression for specific energy depends on the work done while removing a unit volume from the rock (1964). The volume excavated by the indenter was calculated for finding the specific energy by displacing fluid using a burette (Benjumea, 1969).

Dong (2017) described rock indentation in his work with a detailed diagram as shown in Figure 2-4 with a setup that forces an indenter downwards into the rock at a controlled

loading rate with sensors monitoring the load and the corresponding displacements. The type of rock specimen used in this sort of testing is mostly a rock cylinder or a cylindrical disc. A holding device is used to keep the rock intact and avoid its movement. The movement of the upper platen with the indenter is recorded and stored by the sensors. The sensors then send their values through software that generates a plot of loading with Load on the vertical axis and Displacement on the horizontal axis. The test continues until a crater is formed to produce the loading curve which is then analyzed to draw conclusions.

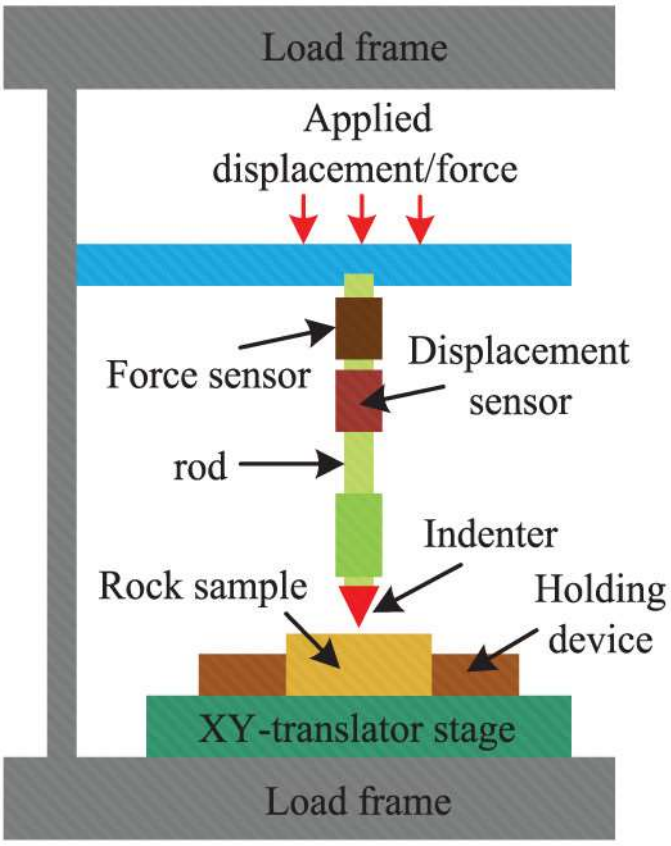

Figure 2-4: Experimental setup of a rock Indentation test. (Dong, 2017)

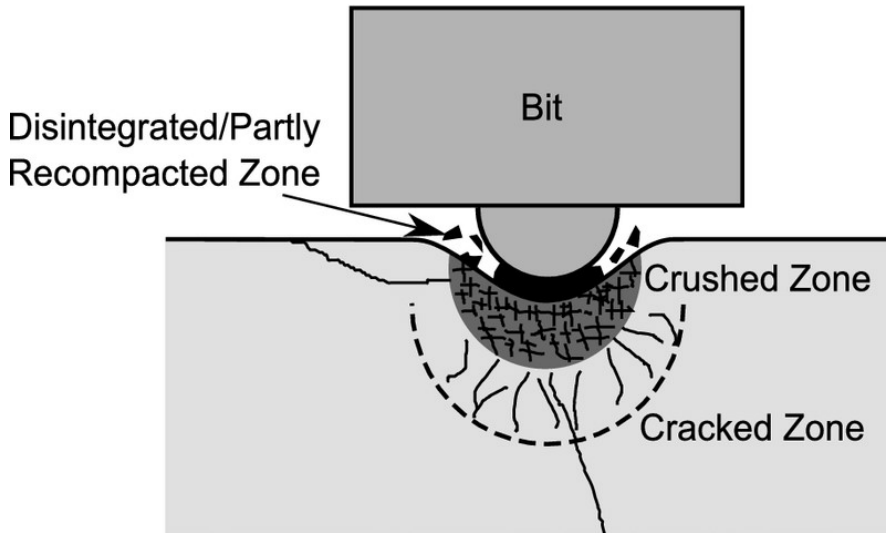

Figure 2-5: Illustration of crack formation from rock crushing by a drill bit. (Song, 2021)

Rock-breaking action done by percussive drilling was studied by Song in the analysis of the drilling performance. There was a comparison made between the rock breakage by laboratory indentation and the type of percussive drilling. The bits execute the cratering phenomenon on a macro-scale compared to what is done on a micro-scale using the apparatus from Figure 2-5 in a laboratory.

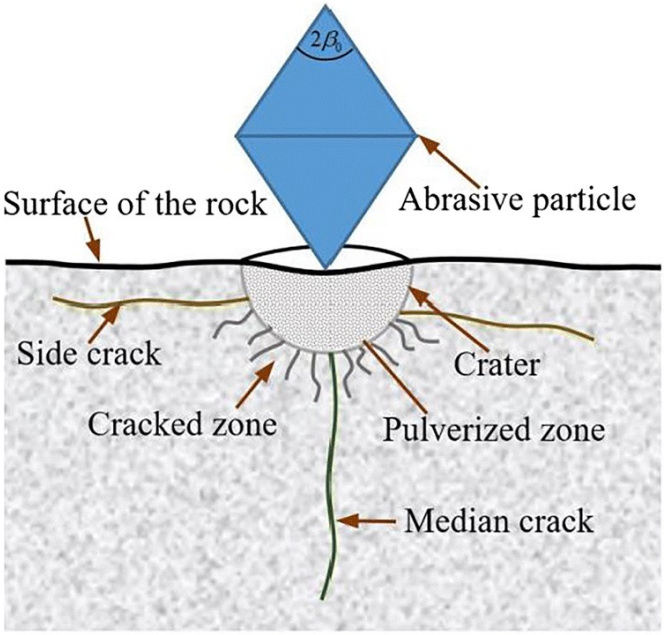

Figure 2-6: Post indentation zones and cracks in rocks. (Fernando, 2020)

In the indentation process, the compacted zone (or the pulverized zone) seals any faults that are in the rock by compacting the pores beneath the indenter. Further from the indented surface is the cracked zone, where the micro-cracks extend into the rock as shown in Figure 2-6.

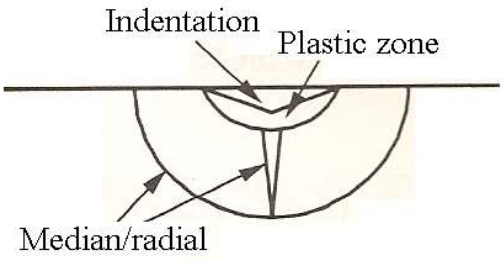

Figure 2-7: Dominating crack and zone after the rock is indented by a tool. (Rocha-Rangel, E, 2011).

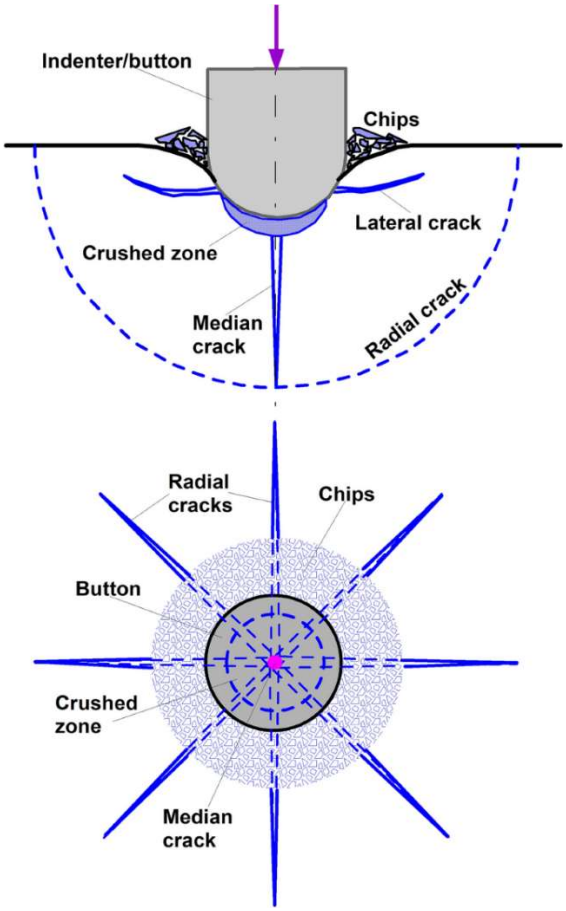

Figure 2-8: Crack propagation top and side view during indentation on rocks. (Zhang, 2021)

Shetty (1985) carried out an investigation on median cracks occurring in rocks when subjected to loading with an indenter normal to the rock surface. In his findings, he highlighted that the median cracks are generated directly under the tip of the indenter and lengthen throughout the rock on the same axis. The length of the median crack displayed a linear relationship with the force of loading applied. In Figures 2-7 and 2-8, the crack propagation and zones created after indentation are presented.

2.2 Principle of Indentation tests

Indentation is an effective method to evaluate the cutting tools in rock breakage processes. The indentation process utilizes a metallic indenter with a hardness of 58 HRC (ASTM standards D5731 – 16). When a load is applied through a servo-controlled system into the indenter, the rock and the indenter are subjected to a stress field. The responses of this stress field are decided by the indenter's geometry and the loading rate at which the normal force is applied through the indenter to the rock. The elastic limit for the rocks are very small compared to metals, and as the load applied consistently increases, the rocks in their elastic range reach their elastic limit, and then the plastic deformation begins. This is the zone where the indenter actually starts penetrating into the bulk of the rock (Murthy, 1998). The test goes through certain stages that could be well explained by a graph of the loading curve; the indentation phase starts with surface crushing and elastic deformation, then the indenter extends the area of the crushing zone, and finally, the test is concluded with the production of chips. The penetration of the indenter is determined by the tool's effectiveness and the dispersion of cracks. The process of indentation leaves three zones below the indenter, the first being the compressed or compacted zone, which closes the defects in the rock. The next zone is the elastic deformation zone or the crushed zone; this zone consumes the main part of the energy of fragmentation. Finally, the cracked zone is the furthest from the indented surface, where micro-cracks travel into the rock (Tan, 1994). The energy consumption of this process depends on parameters such as indenter geometry, the confinement of the rock below the contact surface, and the rocks geomechanical property such as internal friction. Through his own experimentation, Huang (1998)

discovered that shear failure occurs at shallow depths and tensile failure occurs at deeper depths in the indented rock samples.

2.3 Indentation Hardness Index

The loading of the indenter against the rock specimen leads to different phases before the final phase of rock failure. The linear section of the loading has a uniform slope where the maximum load corresponding to the displacement in the rock is called the Indentation hardness index (kN/mm), after which there is a critical transition point where the load drops to form a crater (Hamilton and Handewith, 1970). Szwedzicki (1998) came up with an equation to correlate with the UCS, which is a very important rock parameter:

$$UCS\ (MPa) = 3.1\ X\ IHI^{1.09} \qquad (1)$$

Kahraman (2012) worked on correlating the indentation index to the unconfined compressive strength with a reasonable coefficient of regression:

$$UCS = 0.07\ IHI + 28.28\ R^2 = 0.7 \qquad (2)$$

UCS is for uniaxial compressive strength in MPa and IHI stands for indentation hardness index in kN/mm. There were also correlations for Brazilian tensile strength, but its coefficient of agreement is not as significant (Kahraman, 2012).

2.4 Operating parameters of indentation test

Indentation tests can be conducted using two methods: displacement-controlled system and a load-controlled system (Kalyan, 2016). In a displacement-controlled system, the indenter moves at a predetermined displacement value at every second, perpendicular to the rocks

surface. The second method is the load–controlled system where a certain value of load in Newton or Kilo Newton (kN) is chosen as a maximum value. The test ends when the load on the setup reaches that value previously chosen during the loading curve. These tests have been done using different types of indenters such as spherical, wedge-shaped, and conical indenters, but this thesis deals with only conical indenters for study. There are also no tolerance values for the conditions for sample preparations. Further, the test is significantly affected by some factors that shall be discussed briefly: (1) indenter geometry (Apex angle, Shape of the indenter, and the tip diameter); (2) Loading rate or the strain rate; (3) Confinement of the rock to be tested, and (4) Rock properties.

2.5 Variables affecting the test results

2.5.1 Influence of the Geometry of the metallic indenter

For chipping to occur, the sum of the internal friction angle and wedge angle should be less than 90° (Paul, 1965) and for any wedge angle that exceeds this criterion, the indenter penetrates into the rock without any chipping. Any change in geometry completely changes the stress field in the rock during the test. The standard indenter utilized according to the ISRM draft proposed by Szwedzicki (1998) was similar to the Point load strength apparatus from ASTM standards D5731 – 16 having an apex angle of 60° and a spherical tip diameter of 5mm. The indenter was also manufactured from hardened steel rated at 58HRC. It should be noted that the material selection of the indenter also plays an important role. As the tip diameter of the indenter is increased, keeping all other variables constant, the indentation index increases as well. This means that with a narrower tip, the penetration into a rock compared to a wider tip for the same displacement utilizes less indentation force. (Premraj, 2022)

2.5.2 Influence of the loading rate

The rate at which the indenters move normally towards the rock specimen at a predetermined loading rate has a direct effect on the curve produced. A high loading rate can end the test quickly and would leave us with a substantially smaller linear zone from the loading curve. To make results replicable and consistent, researchers set up a certain loading rate. Szwedzicki (1998) suggested the use of loading rates with a range anywhere between 0.05-0.15kN/sec having concluded that a loading rate anywhere between these values gave results that were consistent and close. Other researchers such as Copur (2003), Mateus (2007), Haftani (2014), and Zhang (2018) used a rate ranging from 0.0025mm/sec to 0.01mm/sec, but they later concluded that using a loading rate between these two values did not lead to significant changes in the results from indentation.

2.5.3 Influence of the confinement subjected to the rock sample

Studies from the past suggest that increasing confinement leads to an increased amount of energy required for breaking rock and increased indentation indices. In terms of graphical representation, the loading curve shifts upwards with a more inclined slope. It is also observed that when subjected to confining stress greater than just the atmospheric pressure, the cracks formed are deeper than without confinement (Liu, 2016).

2.5.4 Properties of the rock

Rocks possess varying physical properties based on their composition so we must go beyond using just geological classification when describing the behavior of rocks. Notably, mechanical and geomechanical properties have an influence on loading during testing. The

loading depends on the physical properties of the rock such as permeability, porosity, saturation, and density. It also depends on mechanical properties such as Young's modulus, tensile strength, poison's ratio, internal friction angle, joints and fractures in the rock, and abrasivity.

2.6 DEM Simulation

The PFC2D is a DEM software that is widely used to solve many geotechnical engineering problems. The PFC2D is used in this study to simulate the mechanical behavior of the rock model, which is considered as an assembly of separate particles bonded together at each contact point. For macro-parameter calibration operations in PFC simulations, a proper selection of micro-parameters of particles and bonds and several rounds of trial and error procedures are required. In this study, the UCS result, Young's modulus, and Poisson's ratio are used as the indicator parameters for the material calibration. The simulation models of the RLM and granite are both established in the simulation.

The chosen bond particle model (BPM) is a parallel bond model that may be thought of as a series of springs with normal and shear stiffness in the particles' contact bond. Tension and torque are produced when particles move in relation to one another. The bonds will break if these forces exceed the predefined strength conditions.

The model creation technique comprises of a packing phase followed by a finalization step. The linear contact model was fitted at all grain-grain contacts during the packing phase, and PFC walls were formed to prevent the balls from escaping from the vessel. The servomechanism also controlled the movement of the vessel walls. Following that, the linear parallel bond model and particle material attributes were assigned to the contacts during the

finalization process and the connected ball assembly was eventually obtained.

When doing a uniaxial compression test to calibrate the micromechanical characteristics of limestone, the model's micromechanical parameters and physical parameters must be supplied. Effective modulus , stiffness ratio, frictional coefficient, parallel bond effective modulus, parallel bond stiffness ratio, mean value of parallel bond normal strength, mean value of parallel bond tangential strength, standard deviation of parallel bond normal strength, standard deviation of parallel bond tangential strength, and radius multiplier are all micromechanical parameters.

Calibration of macroscopic and microscopic parameters must be undertaken first due to uncertainty in microscopic parameters and macroscopic responses. The trial and error method is a popular calibrating method. Xu et al. (2020) carried out a series of PFC rock model calibration tests and proposed the link between the rock model micro parameters to the macro parameters. Elastic modulus is related to effective modulus and negatively related to stiffness ratio. Poisson's ratio is related to stiffness ratio. UCS is related to parallel bond normal strength mean value and negatively related to effective modulus and stiffness ratio.

Chapter 3: Experimental Methodology for Research Related to Indentation Tests

3.1. Introduction

The indentation test is an indirect testing procedure used for estimating the strength of rocks (Kallu, 2015). Similarly, the rock breakage of rock by conical tools in surface excavation procedures follows the same mechanism of breaking the rock as the indentation strength test (Morris,1969), (Kahraman, 2000). Understanding the mechanisms of rock breakage can be linked to penetration rate prediction for drilling tools. The penetration rate is a very important factor as it could be utilized in the economic planning of the drilling or excavation projects. In the process of exploring more about the indentation tests, a detailed investigation was conducted. This thesis deals with two manuscripts – Chapter 4 and Chapter 5 – involving experimental work that was published in International conferences. As an introduction to these manuscripts, this chapter details the aspects of the experimental process conducted. It covers majorly the types of rocks involved in the study, their material properties, the apparatus used for the experiments, and the methodology applied for setting up and performing the experiment.

3.2. Rocks used in experiments

3.2.1. Granite

Granite is the hardest of the rocks used in the experiments for this thesis. Core samples of a diameter of 47.9 mm were cored out of granite blocks. They were cut according to

the required sample dimensions for UCS, ITI, and PLI tests for strength and material characterization in the drilling Laboratory at the Memorial University of Newfoundland. The tests also include finding the elastic properties of the rocks (Quan, 2021). Table 3-1 below summarizes the results from the rock characterization done by researchers at Memorial University.

Table 3-1: Material Characterization results of Granite rock. (Shah, 2020), (Quan, 2021)

Rock Type	Density	UCS	ITI	PLI	E	P-wave	S-wave	Elastic constants	
	(g/cm^3)	(MPa)	(MPa)	(MPa)	(GPa)	(m/s)	(m/s)	E' (GPa)	μ
Granite	2.93	167.78	16.42	14.17	13.17	5480.91	3433.19	81.14	0.18

Where E is the Young's modulus, P and S waves are the primary and secondary waves travelling inside the rock core, and μ is the poisson's ratio.

3.2.2. Medium Strength Rock Like Material (MS RLM)

This synthetic type of rock is a kind of concrete and was manufactured by researchers at Memorial University. The reason for the strength being categorized as medium is due to the lesser water content and greater cement content in the solid mixture (Zhang, 2016). The recipe of the synthetic rock is specified below in Table 3-2.

The entire batch of rock was manufactured in 2016 and left in water tanks to cure as 4-inch by 12-inch cores. These were then cored into the similar dimensions as granite for

testing. The most recent rock characterization tests from 2021 have been recorded in Table 3-3. This rock was half as strong as granite and was used for experimental work for the OMAE manuscript work presented in Chapter 4. The rationale behind the selection of this rock was primarily due to its abundance in the laboratory as well as its strength, which corresponds to medium strength rocks in field conditions such as sandstone. For the experimentation, we therefore had a very hard rock type and a medium strength rock.

Table 3-2: Recipe for Medium Strength rock. (Zhang, 2016)

Materials	**Designed Quantities**	**Used Quantities**
A: C: W	3: 1: 0.45	3: 1: 0.45
Aggregate	30 kg	31.436 kg
Cement	10 kg	10 kg
Water	4.5 kg = 4500ml	3.064 kg = 3064 ml
Water Reducer	N/A	N/A
Superplasticizer	Daracem 19= 60 ml	Daracem 19= 60 ml
Silica Fume	N/A	N/A

Table 3-3: Material Characterization results of Medium Strength rock like material. (Quan, 2021)

Rock Type	Density (g/cm^3)	UCS (MPa)	ITI (MPa)	PLI (MPa)	E (GPa)	P-wave (m/s)	S-wave (m/s)	Elastic constants E' (GPa)	Elastic constants μ
MS RLM	2.3	78.98	6.9	5.79	9.48	4703.85	2840.99	44.98	0.21

3.3. Materials and Equipment for the tests

3.3.1. Servo-control loading frame

Figure 3-1: Servo-control loading frame.

All of the rock indentation tests were performed by a servo-controlled loading frame. The instrument was an Instron 5585 series dual column floor model weighing 2100lbs. The maximum capacity for tension or compression on the instrument is 250 kN and works on the principle of closed-loop servo control. The metallic indenters used in indentation are mounted on the top platen. The compression loading rate is chosen ahead of time and the experiment is run for a span of 3 minutes.

Table 3-4: Specifications of the servo-control loading frame. (M10-14190-EN series, 2005)

Load capacity	**Minimum speed**	**Maximum speed**	**Position accuracy**	**Load measurement accuracy**	**Strain measurement accuracy**
kN	**mm/min**	**mm/min**	**mm**		
250	0.001	500	± 0.02	± 0.4%	± 0.05%

3.3.2. Metallic indenters

Indentation test results are completely dependent on the metallic indenters used, and as experimental work in chapters 4 and 5 had different objectives, the indenters chosen for each experiment were specific to those objectives. To be precise, the tip diameter (D) was the varying parameter of the indenter. The indenters have a spherical tip and, hence, changing their dimensions changes the geometry of the indenter. Two parameters that remained the same for both the studies were (i) the hardness of the indenter and (ii) the apex angle (α) which is the angle between the cone of acceptance and the central axis

passing through the indenter. The hardness of the indenter was 58HRC in the Rockwell hardness scale for metals following the point load apparatus from ASTM D5731-16 and the value of the apex angle was 60°.

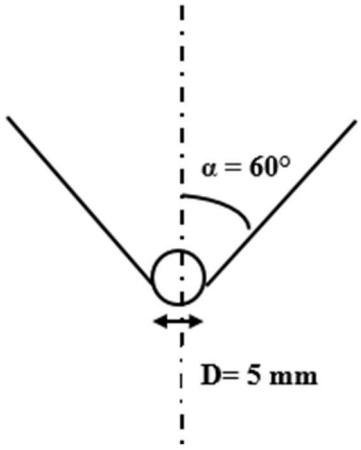

Figure 3-2: Geometry of indenter used in chapter 4.

The tip diameter of 5 mm was utilized for the research done, as shown in Figure 3-2. This is the exact same metallic indenter that was used for the point load strength testing. On the other hand, chapter 5 deals with indentation test responses based on variables involved in the experiment. The geometry of the indenter, for example, plays a big role in rock fracture and its responses (Thiercelin, 1988) (Uboldi, 1999). Hence, tip diameter influence was chosen for study. In Figure 3-3, the three indenters are arranged in ascending order (from a to c) of increasing tip diameter.

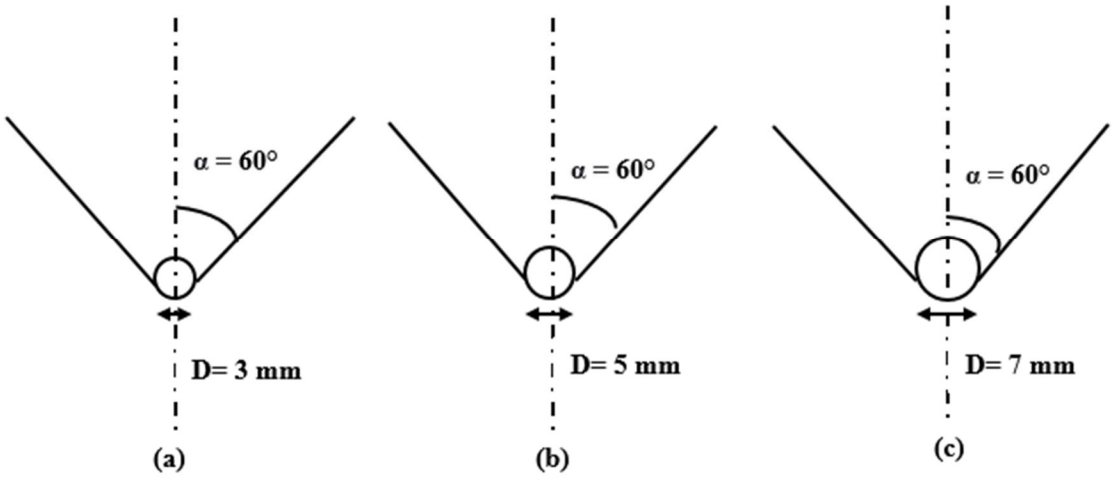

Figure 3-3: Indenters used for studying the influence of tip diameter in chapter 5.

3.3.3. Metallic straps

The confinement around the rock cores were created using a metal strap that was manufactured by the technical services at Memorial University as displayed in Figure 3-4 and 3-5. The two ends of the straps were connected to one another by a nut and bolt assembly. Tightening the bolt brought the two ends of the straps together around the circumference of the rock core and thus acted as confinement.

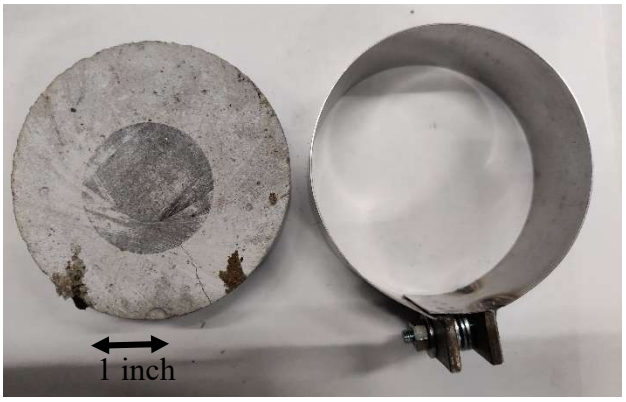

Figure 3-4: Metal strap used for research in chapter 4.

Figure 3-5: Metal straps used for research in chapter 5.

3.3.4. Torque wrench

Figure 3-6: Torque wrench. (Duratool manual)

The study of confinement was a part of work from chapter 5. The metallic straps secured with bolts were tightened using a torque wrench to provide confinement to the rock core sample. The instrument in Figure 3-6 provided a range from 1 - 15 Nm torque values. It has a tolerance of ± 10%. Chapter 4 used confinement around the sample with a value of 8.48 Nm and in chapter 5, two values of 7.35 Nm and 8.48 Nm were applied. The conversion of the torque into equivalent pressure is complicated as it involves friction and stiffness of metal. The work utilized the torque values but it can be concluded that

the conversion of torque to pressure is a long-term goal. Careful tightening of the bolt to a required torque level will result in a clicking sound, signifying that the wrench will not tighten anymore. The rationale behind the selection of the two confinement levels was to incorporate comparison amongst confinement levels. 8.48 Nm confinement was the maximum torque value at which the two ends of the metal straps were closest to each other. For values below 5 Nm, the core slipped between the metal straps, and at 6Nm, the core was engaged with the strap. With this information, 7.35Nm, a value a bit further from 6Nm, was chosen as the first confinement level.

3.4. Specimen preparation

3.4.1. Specimen preparation for chapter 4

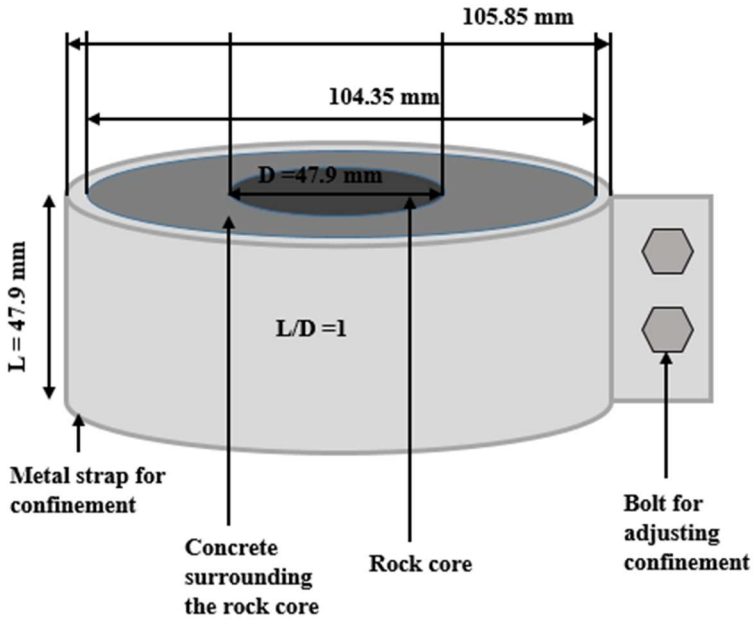

Figure 3-7: Dimensions of the sample for indentation in chapter 4.

From Figure 3-7, we can comment that the sample preparation for this work involved

cutting a core of rock to the dimensional criteria of a length to diameter ratio of 1. The ends of the core were also flattened and smoothened using a grinder. This sophisticated procedure was followed using the ISRM draft for indentation testing on rocks (Szwedzicki, 1998). The core was surrounded by concrete in a 4-inch diameter mold and cured for 2 days at room temperature. The average strength of the mold was approximately 30-35MPa. The cured concrete holding the rock core was taken out of the plastic mold and a customized metal strap was positioned around its circumference. This study utilized two kinds of rocks; namely granite and medium-strength rock-like material.

3.4.2. Specimen preparation for chapter 5

The specimens for this study required less preparation. First, the cores were retrieved from large granite blocks and the ends were flattened and smoothened using a grinder. There were two types of core samples used for this study that were differentiated by their length-to-diameter ratio: 0.5 and 1 as displayed in Figure 3-8. Notably, the metal straps around the cores were customized, augmenting the confinement-based indentation tests on samples. In addition, the bolts were tightened using torque wrenches at selected torque values to provide confinement around the rock samples.

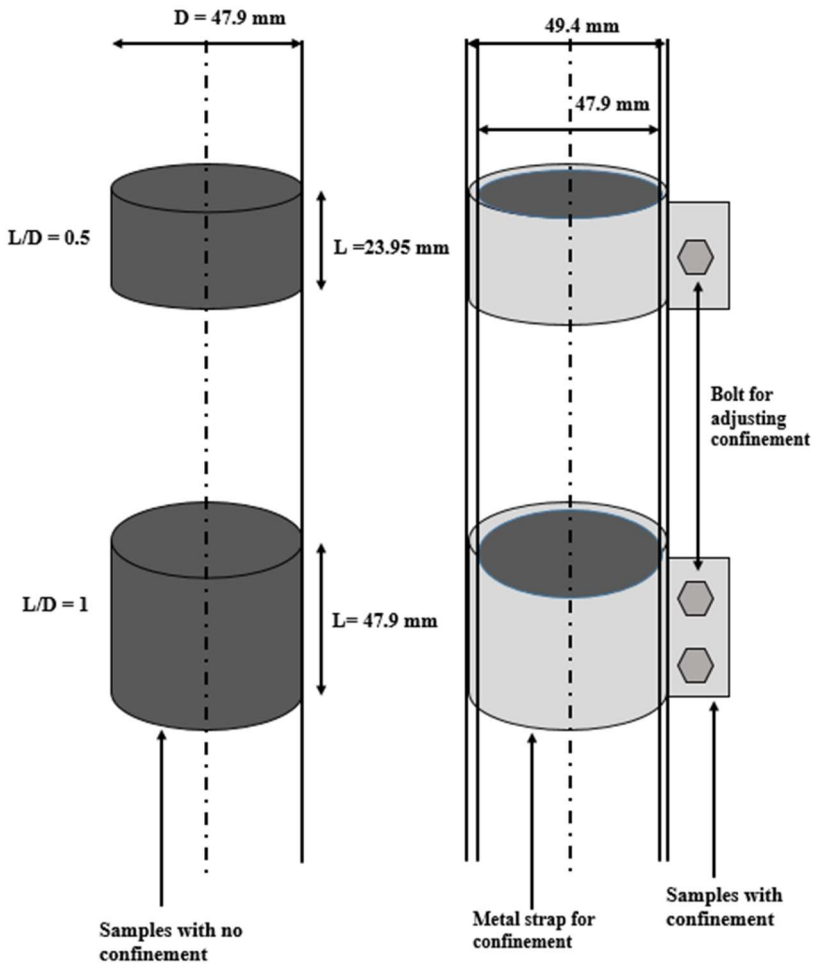

Figure 3-8: Dimensions of the sample for indentation in chapter 5.

3.5. Methodology adopted for the testing procedure

3.5.1. Initiation of the test

The following checklist is to be completed for the test in order to achieve replicable results.

- The sample preparation is completed and the samples have flat ends.
- The loading frame is calibrated and setup at the required loading rate.
- The indenter is connected to the top moving platen of the loading frame by threads and is held tight using rubber strap wrenches. (This ensures that the loading curve does not have any strain from indenters' loose threads.)

- The indenter is pressed against the sample at a load of 12 Newtons. (This is for engaging the rock sample - having all the tests start from the same value ensures repeatability.)
- The test can begin at the predetermined loading rate for a duration of 3 minutes.

3.5.2. Loading rate type and range selection

The indentation test is sensitive to loading rate. This is important to note as it means that if the loading rate changes, so will the results. There are two types of loading: load-controlled and displacement-controlled (Kalyan, 2015). The load-controlled loading is where a predetermined load is applied per unit second on a sample. When a rock fails or fractures, the load drops. In such situations, the system will ramp up which is a big disadvantage of this loading type. On the other hand, displacement-control loading results in a series of small rock breakage patterns before failure as the indenter is displaced at a uniform rate into the rock. With this knowledge, most of the researchers in past have been using displacement-controlled loading. In this type of loading, the indenter is planned to displace itself by a unit distance every second. This is suited to rocks of all kinds of strength.

Various researchers have also used a loading rate value of 0.001mm/sec repeatedly. The changes in results of indentation using loading rates between 0.0025mm/sec and 0.01mm/sec are not significant (Zhang, 2018).

3.5.3. Analysis of the results

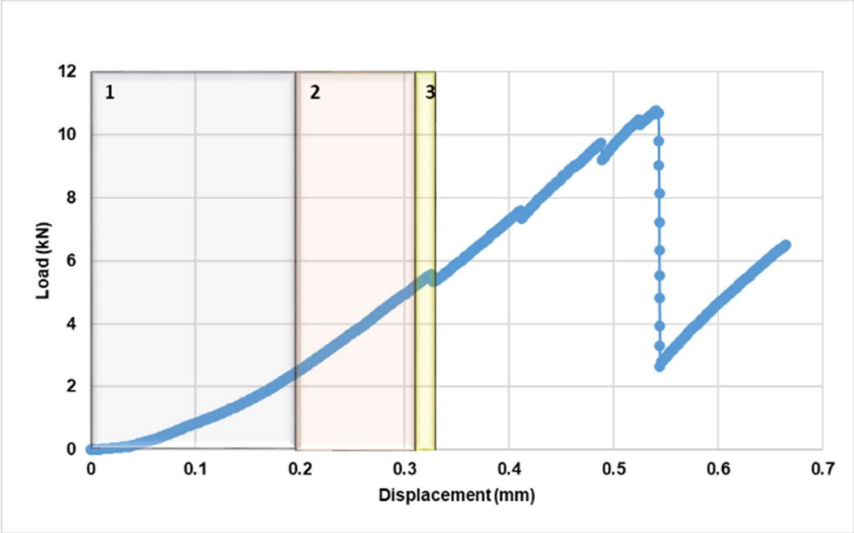

Figure 3-9: Plot of the indentation test for analysis. (Premraj, 2022)

The curve from Figure 3-9 represents three highlighted zones numbered as 1, 2 and 3 respectively. Zone 1 is the elastic region of the loading curve and is the zone of non-linearity. The harder the rock gets, the smaller the area becomes.

Zone 2 is the important part of the linear section of the curve as it is used in the calculation of slope for finding the indentation hardness index (KN/mm). Finally, zone 3 is where the rock is cratered by the indenters compressing action. These three zones occur as a cycle which repeats until the rock finally splits into two pieces.

The servo-controlled device has a very high sampling rate and thus the points on the plot are densely populated. There can also be some amount of noise, but this can be eliminated by smooth averaging of the data in Microsoft excel.

3.5.4. Estimation of crater volume post indentation

The metallic indenters used in this experiment have a spherical tip. The tips for the study in chapter 5 were 3mm, 5mm and, 7mm respectively. When the indenters were forced against the rock, the tip creates a concave impression known as a crater. The volume of the crater is thus the volume of the sphere that occupies the crater represented in Figure 3-10.

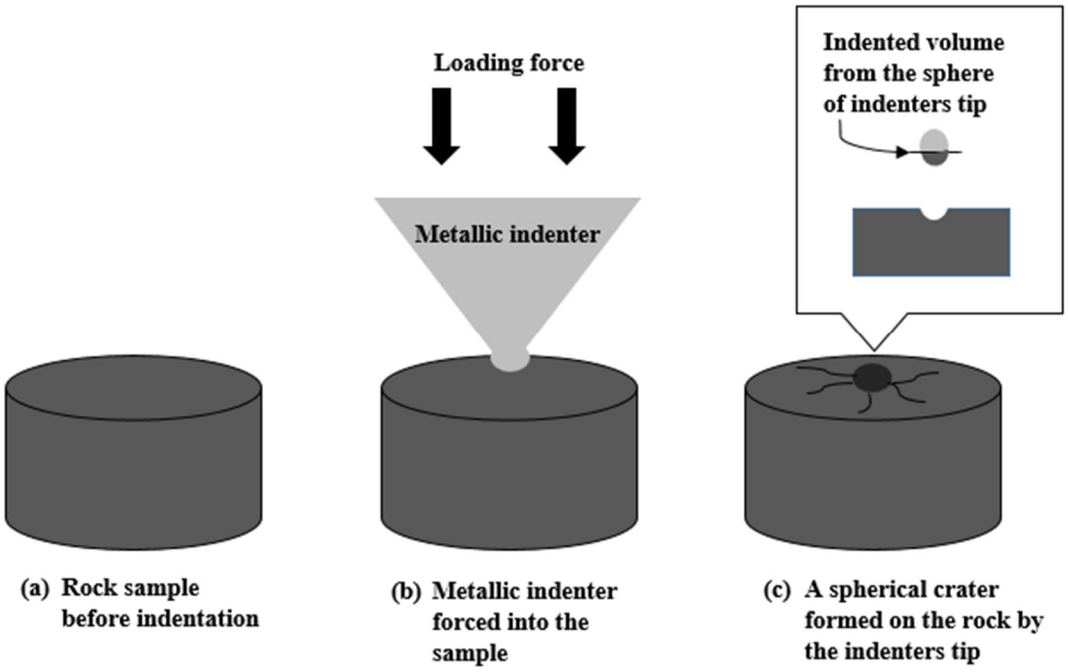

Figure 3-10: Representation of a spherical crater formed by the tip diameter of the indenter.

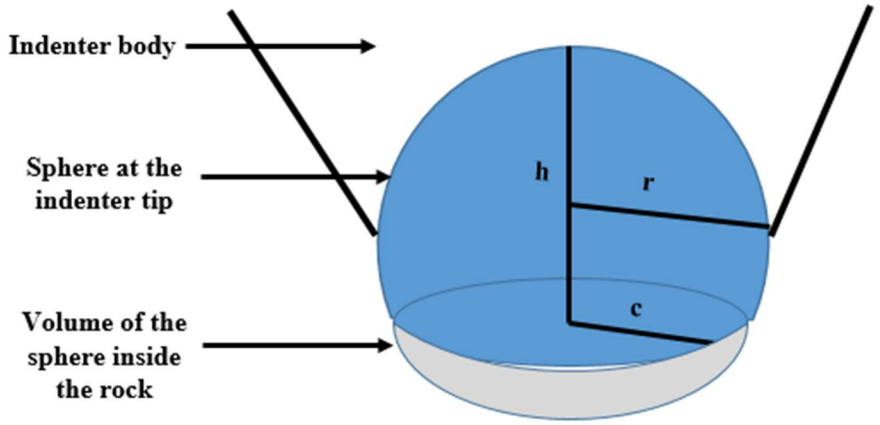

Figure 3-11: Explanation for indentation volume calculation.

To calculate the volume of the crater, the volume of the grey highlighted zone from figure 3-11 must be determined. In Figure 3-11, (r) is the radius in mm, (h) is the height which is diameter of the sphere minus the indented depth in mm, and c is the radius of the bottom. To calculate the volume of the indented zone, the radius of the bottom is calculated.

The following formulas are required in the process of crater volume calculation:

$$C = \sqrt{[h\,(2r-h)]}$$

$$V \text{ partial} = V = \pi/6\; h(3c^2+h^2)$$

Where π is 3.14, V partial is the volume of the blue shaded zone in the sphere (mm^3)

3.5.4.1. Procedure for calculating crater volume

- The point on the plot from Figure 3-9 where the crater forms is selected; this is the point after which there is a fall in the compressional load.

- Corresponding displacement value is noted from the data in Microsoft excel.
- Height (h) is then calculated by taking that displacement value and subtracting the value from the diameter of the sphere.
- Use the formulas to find the radius of the bottom part (c) of the image.
- Substitute the value of (c) in the formula for volume and calculate the volume of the sphere which is not indented into the rock surface and call it (V partial).
- Calculate the total volume of the same sphere and call it (V total)
- Subtract (V partial) from (V Total); this gives you the volume of the sphere indented which is equal to the volume indented.

3.5.5. Specific energy calculation

Specific energy is the energy required by a tool to excavate unit mass. This parameter tells a lot about tool performance. In chapter 5, specific energy study has been performed on varying tip diameters in the indenter and the confinement around the rocks. The specific energy in non-rotary rock breakage by indentation is the ratio of the work done to the volume excavated (Teale, 1964).

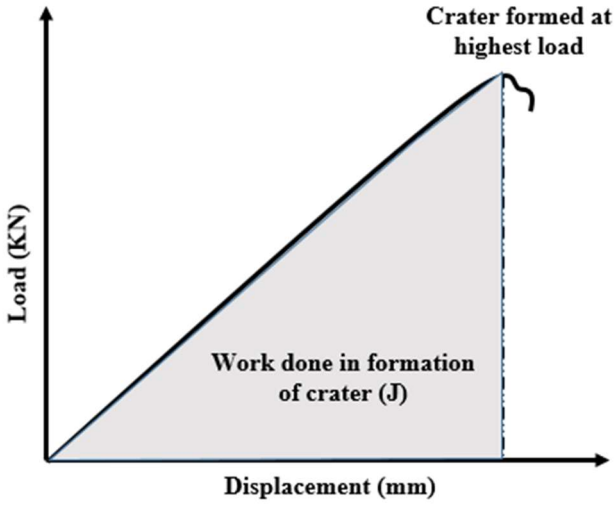

Figure 3-12: Plot highlighting shaded region as the work done in cratering the rock.

3.5.5.1. Procedure for calculation of specific energy in rock indentation

- The point on the plot form Figure 3-9 is selected where the crater forms; this is the point after which there is a fall in the compressional load.
- Corresponding displacement value is noted from the data in Microsoft excel.
- Using Microsoft excel, perform an integration of the points under the curve in the shaded region from Figure 3-12.
- Calculate the volume of the crater using the displacement reading at crater formation.
- Divide the calculated work done by the volume of the crater which gives you the specific energy.

Chapter 4. Indentation Test Implementation for Rock Strength Correlation by Experimental Method and Simulation Using Distinct Element Method

4.1 Introduction

The rock beneath the surface differentiates itself based on its characteristics such as texture, color, etc. But one of the most important parameters that put rocks into different categories is the strength of the rock. It helps engineers to predict the rate of penetration during drilling activities by the oil and gas or mining sector. Conventional testing of the rocks follows standard procedures which require rock samples to be made with a high degree of precision. This makes the process time-consuming and difficult. Researchers have found indirect techniques to predict the strength of rocks with less sophisticated sample preparation (Kallu, 2015). The indentation test happens to be one of these tests. The test procedure is followed by forcing a conical metal indenter against a rock core. The loading curve produced from this test is used in predicting strength of rocks using empirical correlations (Szwedzicki, 1998). This study uses two types of rocks, namely concrete of medium hardness and granite which is very hard. The main focus of the study was primarily to predict the rock strength. Secondarily, the experimental indentation was duplicated numerically using a DEM (Distinct Element Modelling) software called PFC2D. The modelling software helps us understand the failure pattern that the cannot be visualized in the laboratory due to the opaque nature of the rock. It

also produces a loading curve that is similar to the experimental results (Zhang, 2018). This publication work was made possible by the combined efforts of a dedicated team. Dr. Stephen Butt has supervised the authors during the experimental work and composure of the paper. Dr. Abdelsalam Abugharara organized a sophisticated experimental plan to perform the tests in the best way possible. Zijian Li generated the code for the DEM modelling and assisted in performing the experiments in the laboratory and data processing. Prajit Premraj developed a plan for the experiments, prepared samples, performed the tests, compiled and analyzed the data to make comparisons between experimental and simulation results, and wrote the manuscript.

4.2 Indentation Test Implementation for Rock Strength Correlation by Experimental Method and Simulation Using Distinct Element Method (Manuscript #1 from OMAE 2022 conference organized by ASME)

Prajit Premraj, Zijian Li, Abdelsalam Abugharara, Stephen Butt

Memorial University of Newfoundland, Department of Process Engineering, St. John's, Newfoundland

Abstract

Rock strength is an important parameter for the drilling penetration estimation, which is usually determined through standard destructive strength tests, which are known to be sophisticated, expensive, and time-consuming. In addition, the accuracy of these tests has a high standard on the rock sample dimension. As a non-conventional method, the rock indentation test is reviewed and conducted in this study to solve these problems.

The sample preparation and test method of the rock indentation test are validated to standardize the test. Based on the stress-strain behavior of the test samples, the correlation between the rock indentation hardness index (IHI) and the rock UCS strength is developed based on different lithology. Then the rock indentation test is simulated in the distinct element method (DEM) in PFC2D software. The robustness of the DEM simulation is validated, and the sample failure pattern is studied. The significance of the process is that it very closely matches with the process a rock fails under the cones of a roller cone drilling bit penetrating the rock.

Keywords: Drilling penetration; nonconventional; indentation test; simulated; failure pattern.

4.2.1. Introduction

The paper aims at performing tests for indentation and use of the IHI to find the unconfined compressive strength of rock. As the paper also deals with a numeric aspect using DEM simulation along with the experimental method, a rock characterization had to be done to input the rock parameters into the simulation model. Swain et al added that rocks are complex structures and are opaque so any test on them is restricted to before and after external visualization studies (Swain, 1976) . It tells about the drilling property and crushing behavior but doesn't deal with the modes of failure. Indentation hardness test is an indirect method and can be used to correlate with the unconfined compressive strength as they have a linear relationship for specific rock types from the previous studies and experimental work carried out by T.Szwedziki (1998) et al . Kahraman (2012) et al investigated the relationship between

Indentation – load curve and rock properties to develop prediction models for drilling. A standard IHI test was suggested by ISRM that predicted UCS from the IHI (T.Szwedziki,1998).

$$UCS = 3.1\ IHI\ \hat{}1.09$$

Where UCS is the unconfined compression strength in MPa, IHI is the Indentation hardness index from Indentation tests in kN/mm and is the highest point where maximum displacement of the indenter is achieved on the application of a maximum load thereafter which any increased load craters into the surface of the rock and slumps down the curve.

Studies say that the Indentation index of moderately hard rocks was in the range of 20-30kN/mm while harder rocks have a range from 40-50kN/mm in their IHI. The procedure for the indentation test involves using a servo-controlled loading frame. This system can provide a load on a disc sample with a conical indenter attached to it with an apex angle of 60degree and a 5mm tip diameter (T.Szwedziki, 1998). The loading rate from 0.025-0.01 has no significant influence on the indentation index of the rock. The tip diameter of the indenter did play a role as the larger diameters gave a higher indentation index while the smaller diameters gave a comparatively lower value of the indentation index (Haftani, 2015) .On loading with an indenter, the rock sample has a chance to split into two pieces rather than just forming a crater. Therefore indentation samples are surrounded by a plaster material so that the rock does not split apart when subjected to loading and rather forms a crater. This in turn duplicates the scenario of rock drilling as they are confined by several layers of rocks. The

confinement leads to increased indentation force and energy (Liu, 2017).

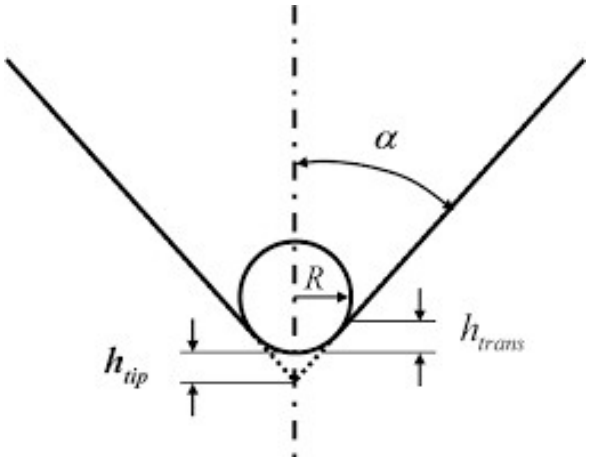

Figure 4-1: Geometry of the indenter for the test. (T.Szwedziki, 1998)

In the above Figure 4-1, α is the apex angle which is 60°, and R is the tip radius which is 2.5mm. Entacher (2014) et al found that UCS values in less brittle formations from indirect tests do not give accurate results . This paper, therefore, deals with rocks of medium hardness to very hard types of rocks.

But the geometry of the indenter plays a crucial role as different geometries can come up with different failure mechanisms and varying rock responses (Thiercelin, 1998), (Ubodi, 1999) Huang (1998) concluded experimentally from his work that shear failure happens for smaller depths and tensile failure occurs for larger depths of penetration in the rock samples indented.

The indenter breaks rather than cutting a solid used for the surface hardness testing can be used for the study of a specific energy that is the removal of a unit volume of rock fragment when subjected to a certain amount of energy. This is important as the specific energy is equal to the strength of the rock if the mechanical efficiency is unity

(Maurer, 1962), (Teale, 1965). Mechanical excavation in the process of drilling is done in two ways i.e. shearing on soft to medium formations and indentation on medium to hard formations. Indenters break rock by applying force normal to the rock surface. While drag bits apply force parallel to the rock surface. Thus, roller cones, disc cutters, percussion tools break rocks by indentation. The process of indentation and the rock failure from that is effective in assessing drill machine performance. The phase of indentation begins with crushing on the surface and elastic deformation followed by extension of crushing zone by indenter and ends with the formation of chips. The indenter's penetration is related to the efficiency of the tool and cracks distribution.

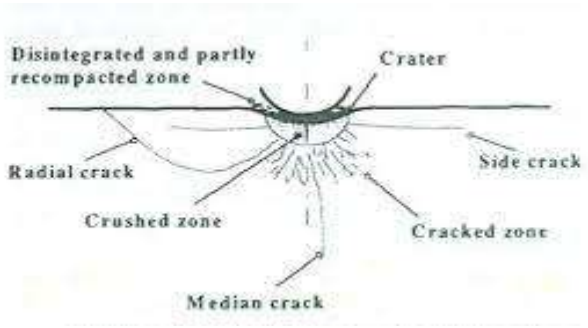

Figure 4-2: Fracture system in rock under indentation. (Tan, 1994)

As illustrated in the Figure 4-2, the process of indentation leaves three zones below the indenter namely the compacted zone that causes closure of the flaws that existed in the rock. There is a crushed zone below that is the elastic deformation zone and further away from the indented surface is the cracked zone where the micro-cracks travel into the rock (Tan, 1994). Predicting the mechanical properties of the rock from drilling rates would be a help to engineers to control changing formation characteristics. These Mechanical properties of the rock, such as UCS, have a significant impact on the design of rock engineering projects (Santarelli, 1996). In the

wellbore stability evaluation, UCS is usually considered one of the most critical parameters compared with wellbore stability compared to other parameters, for example, slope and azimuth (Mateus, 2007). There are two measures established to find the UCS: the standard laboratory tests developed by ASTM (1984) and ISRM (1979) (Singh, 2012). The direct UCS test sets a high requirement on the rock core sample: The sample should be free from planes of weakness, discontinuities, and micro-cracks. In addition, the retrieving of the intact core sample enhances the expenses and to avoid the difficulties in the sample preparation, unconventional methods to derive the rock UCS are deployed. Unconventional tests can be done on smaller samples to derive the UCS of the rock core. As one of the unconventional tests, the indentation test is implemented in the laboratory (Thiercelin, 1998). This article deals with performing strength tests on the rock samples available in the Memorial Universities Drilling lab that is the rock-like material and Granite rock. Tests include conventional and unconventional strength identification tests on standard-sized samples abiding by the standards of the ASTM (American Society for Testing materials) and following procedures underlined by ISRM(International Society of Rock mechanics). Most of the tests are going to be performed on a servo control loading frame at Memorial University that is a fully automated device and provides a real-time plot of the loading of the experiment. As the indentation of rocks has followed varying steps in different studies the work here also tries to propose a certain way to perform the test so that the experiments are repeatable and consistent. In addition to the laboratory experiment, the Finite Element Method (FEM) was also utilized in the rock indentation study (Huang, 1947), (Carpinteri,, 2005), (Paluszny,

014). The Discrete Element Method (DEM) was used to explore the fundamental failure processes that emerge from the rock indentation, as well as the effective factors that influence failure mode (Huang, 1947). The PFC2D software was used to analyze the influence of rock joint angle and rock strength on the fracture propagation pattern induced by rock indentation (Zhang, 2018). By implementing the indentation tests on the two rock types we can make a conclusion on how we can relate to the compressive strength of the rock through the slope of the indentation curve generated from the loading frame. Supporting details highlight the relevance of the work as the experimental work satisfies the actual material characterization done by standard tests in the past and is regenerated using the distinct element modeling code.

4.2.2. Material And Methods

4.2.2.1 Servo controlled loading frame

The servo control frame at Memorial universities Materials lab has a max loading capacity of 250kN. It can perform compressive and tensile strength tests under predetermined custom loading rates, either controlled by displacement or load. In this study, the displacement control loading is applied to avoid the erroneously fast indentation, which induces a large fracture propagates in the rock sample. According to the previous laboratory work, the predetermined loading rate for the test is 0.01mm/sec. 0.005- 0.01mm/sec (Mateus, 2007), (Haftani, 2014), (Copur, 2003), (Haftani, 2013). This is because faster loading may cause the rock to split before cratering process is observed.

Figure 4-3: Servo controlled loading frame.

4.2.2.2 Indentation indenter

Figure 4-4: Indentation indenter.

The test follows the ISRM standards for the Indentation test (Szwedzicki, 1998) according to which the indenter has an apex angle of 60° and a tip diameter of 5mm.

Based on the ASTM standards D5731 – 16 for the Point load index strength test, the indenter strength needs to be no lower than Rockwell 58 HRC.

4.2.2.3 Rocks for testing and their characterization

This article discusses the following rock types: Granite and rock-like material. RLM is a rock-like material made from a recipe for concrete devised by the researchers of Memorial University (Zhang, 2017). The rocks went through UCS tests, Tensile strength test, point load strength, and pulse velocity test following the ASTM standards: ASTM D7012-10, ASTM D3967-08, ASTM D5731-16, and ASTM D2845-08.

4.2.3. Experimental Work

4.2.3.1. Sample preparation

The sample preparation for the indentation test process follows a sequence:

A 2-inch core bit is used to drill a sample into blocks of respective rock samples for study. The cored cylinder is then placed at the center of a 4-inch plastic mold surrounded by wet cement. Following the draft for the ISRM standards for indentation test, the strength of the concrete should be 30-35Mpa. The mold went through a shaking procedure so that bubbles entrapped within getting released from the slurry and to prevent the voids within the material. The mixture is allowed to cure for two days at room temperature. The sample size is subjected to a required dimensional ratio for the diameter and the length of the cylindrical core. After curing, the samples are cut out of the plastic mold and saw cut to a dimensional requirement of Length: Diameter ratio of 1:1 (Kahraman, 2012). The ratio is based on the dimensions of the

rock core to study and not the outer diameter of the concrete cylinder or the metal strapping. The sample is finally metal strapped by a customized metal bracket system that holds it tight and prevents any breakage when high loads get applied on the sample. The outer diameter of the prepared sample core is such that it sits flat exactly on the lower platen with the indenter right on top of it. A calibrated torque wrench is used for securing the core concrete cylinder. The bolts enclosing the metal strap were tightened to a value of 8.84 Newton meters. This value ensures that the sample is held tight between the metal strapping. Constant confinement was provided for all the experiments performed. The purpose of applying the metal strap is to protect the sample from failing or breaking under loading, while the objective is to create a crater and not a fracture.

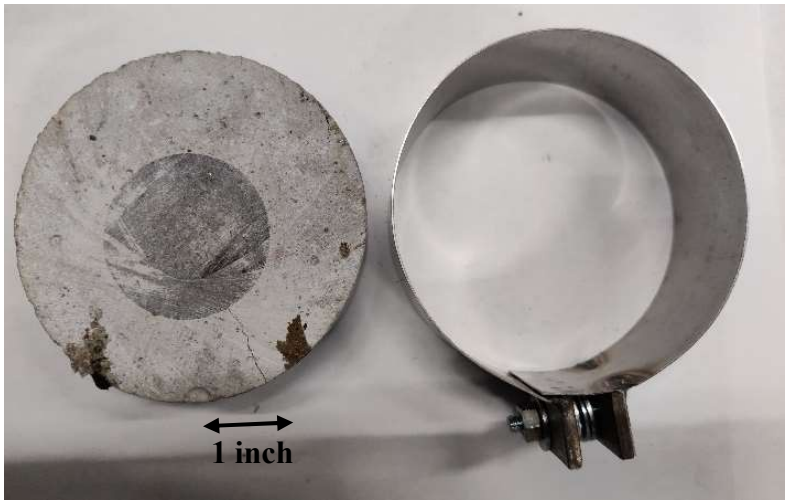

Figure 4-5: The rock sample enclosed in concrete confinement and the metal strapping used for near-rigid confinement.

Figure 4-6: Dimensions of the indentation sample.

After the samples are prepared following the steps highlighted before, they are ready to undergo the indentation test under the static point contact loading by the ASTM suggested indenter that gets connected to the upper grooves of the loading frame. The experiment is displacement controlled (Kalyan, 2015). The prepared sample with a smooth surface and flat ends is centered on the lower platen of the loading frame. The core platen is placed right beneath the rock concrete structure just below the core surface so that the loading is experienced by the rock alone. The indenter is moved to a contact force of 15 Newtons so that we know that the surface and indenter contact is made following which the servo-controlled loading frame begins to displace the indenter at 0.01mm/sec. The experiment is planned for 3 minutes which means the total penetration of the indenter into the rock is 1.8mm.

4.2.4. Results And Discussion

4.2.4.1. Effect of confinement around the rock samples

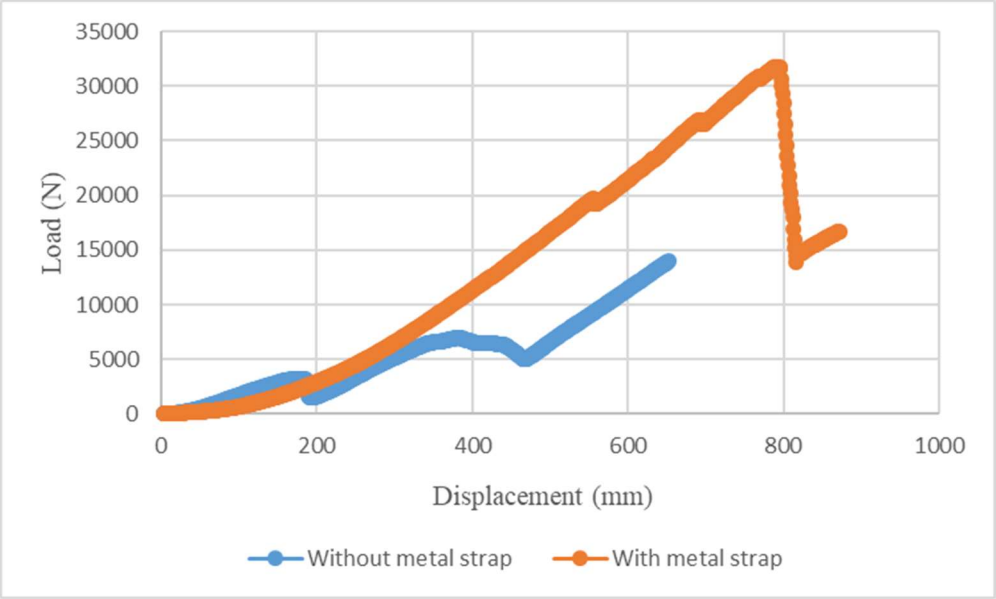

Figure 4-7: Indentation test with and without confinement.

The experimental results portray a significant difference in the indentation curve due to the confinement by the metal strap. The absence of the strap leads to the rock's failure at 3-kilo Newtons at a displacement of only 200 millimeters while the confinement delayed the failure by crater formation. The rock did fail near 30-kilonewtons with the confinement around it and the indenter displaced 800 millimeters. This means that with the metal confinement around the samples, the rock only splits on loading with a value 10 times the value of loading without confinement. The displacement of the indenter into the confined rock was 4 times more than the experiment conducted without confinement.

4.2.4.2. Experimental results on granite

Granite in this study has an average UCS value of 167.78 MPa (Shah,2020) which is higher than the RLM. Its strength comes from its igneous sources and fine grain distribution in its whole volume. Prikryl did a precise rock characterization of multiple granite types and gave a range of porosity from 0.88% to 3% and the grain size average was 0.35mm (Prikryl, 2001). The compact structure of these tiny particles gives granite high strength.

Six Indentation tests were performed on the granite samples, and an average value of IHI generated from the curve was 41.79 kN/mm. We tried to correlate the indentation hardness index to the compressive strength of the rock from the equation suggested by ISRM draft (Szwedzicki, 1998). The equation has a coefficient raised as a power to the indentation hardness index. We call it IT or indentation test coefficient. The value of the coefficient in the equation was 1.09. Some modified IT coefficients were substituted in the formula that gave a rock strength value very close to the experimental results.

Table 4-1: The results of experimental indentation on granite.

			IT Coefficient		
Rock type	Parameters	Slope (kN/mm)	1.09	1.08	1.07
Granite	Avg. UCS	41.798	181.31	174.67	168.27
	Std. Dev.	6.863	29.43	30.8	29.42

Graphical Analysis:

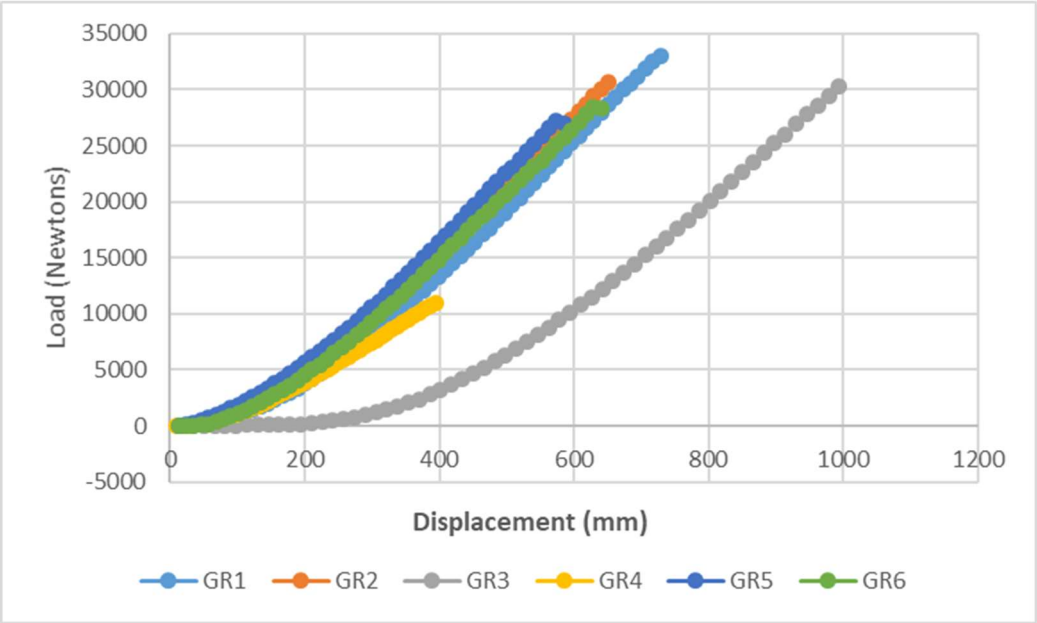

Figure 4-8: Plots for indentation of all 6 granite samples.

The loading is initiated with an elastic deformation, but due to its brittle nature, the penetration of the indenter is no longer reversible, and we can hear a popping sound. The plots depict only the portion until the crater formation where the linear graphical part is utilized to find the slope.

4.2.4.3. Experimental results on rock-like material

The RLM was a synthetic rock made with a specific recipe and thus achieved a predetermined UCS value. Quan (2021) performed some UCS tests on the same samples used for this experiment where the average value was 78.98MPa. The porosity of the RLM is proved to be 7.25%, and the average grain size in the rock is 0.71mm (Zhang, 2017)

Table 4-2: The results of experimental indentation RLM.

			IT Coefficient		
Rock type	Parameters	Slope (kN/mm)	1.09	1.08	1.07
Granite	Avg. UCS	19.615	79.48	77.15	74.89
	Std. Dev.	1.007	4.45	4.28	4.12

Graphical Analysis:

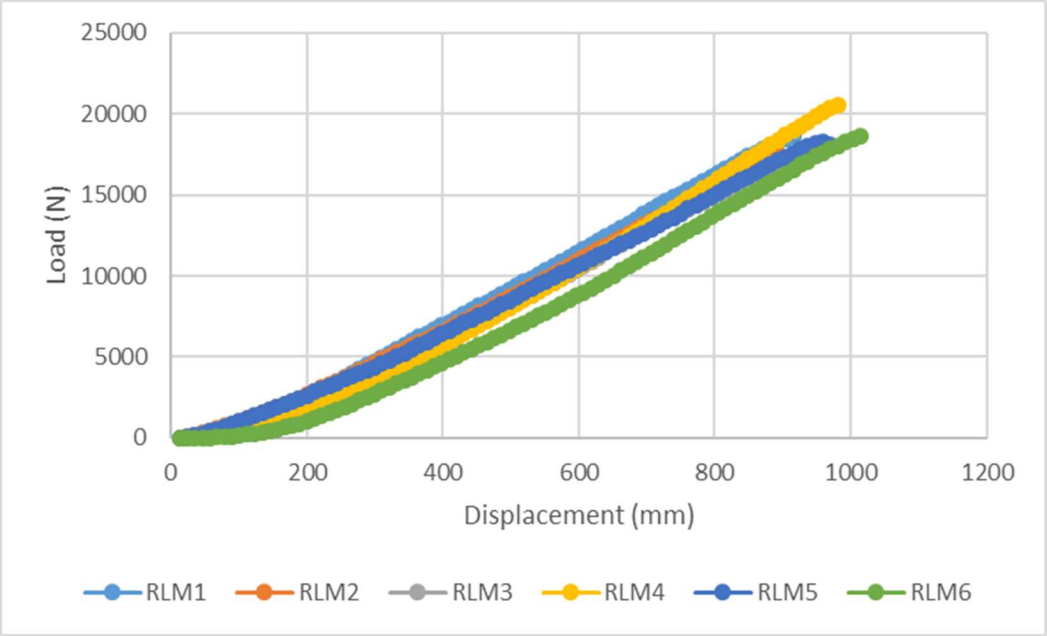

Figure 4-9: Plots for indentation of all 6 rock-like material samples.

Graphically we can see that the displacement corresponding to the IHI for this plot is higher than the granite sample indentation. The average value of the IHI for the MS RLM came to be 19.615 kN/mm. Similar to the correlations made for granite, the rock-

like material too has a new correlation with a slight modification in the coefficient in the formula devised by the ISRM draft.

We can say that as the porosity of the RLM is almost 3.7 times that of the granite, and the particle sizes are twice that of the granite sample, the IHI in Granite is higher than the RLM.

Figure 4-10: Top view of crater formed on an indentation sample.

Figure 4-11: Side view of crater formed on an indentation sample.

Figure 4-12: All rock samples post indentation test.

4.2.4.4. PFC2D simulation results

The PFC2D is a DEM software that is widely used to solve many geotechnical engineering problems. The PFC2D is used in this study to simulate the mechanical behavior of the rock model, which is considered as an assembly of separate particles bonded together at each contact point. For macro-parameter calibration operations in PFC simulations, a proper selection of micro-parameters of particles and bonds and several rounds of trial and error procedures are required. In this study, the UCS result, Young's modulus, and Poisson's ratio are used as the indicator parameters for the material calibration. The simulation models of the RLM and granite are both established in the simulation. The macro mechanical properties of the laboratory result and the simulation result are compared in the following table.

Table 4-3: Comparison between experiment result and simulation result of rocks macro strength.

Material	Data Type	UCS (MPa)	Young's Modulus (GPa)	Poisson's Ratio
Granite	Experimental	167	13.17	0.18
	Simulation	159	14.31	0.17
RLM	Experimental	79	9.48	0.21
	Simulation	81.8	10.17	0.21

The simulation visualization result of the RLM indentation test is given below in Figure 4-13. The rock model consists of yellow particles and the gray particles represent the

cement outside the rock to be tested. The sample is surrounded by two walls representing the metal strap of the sample. The blue indenter is controlled to travel downward to make the indentation. The downward moving indenter crushes the rock. Due to the confinement of the walls, no major crack is formed, splitting the sample during the indentation process. In the top part of Figure 4-13, the black line represents the compressive contact force between particles and the red line represents the tensile contact force. In the bottom part of Figure 4-13, the black line represents the compressive micro-fractures between particles and the red line represents the tensile micro fractures. It is observed that the stress concentrate at the near-indenter zone and the plastic deformation region is formed. The granite simulation result exhibits a similar failure pattern.

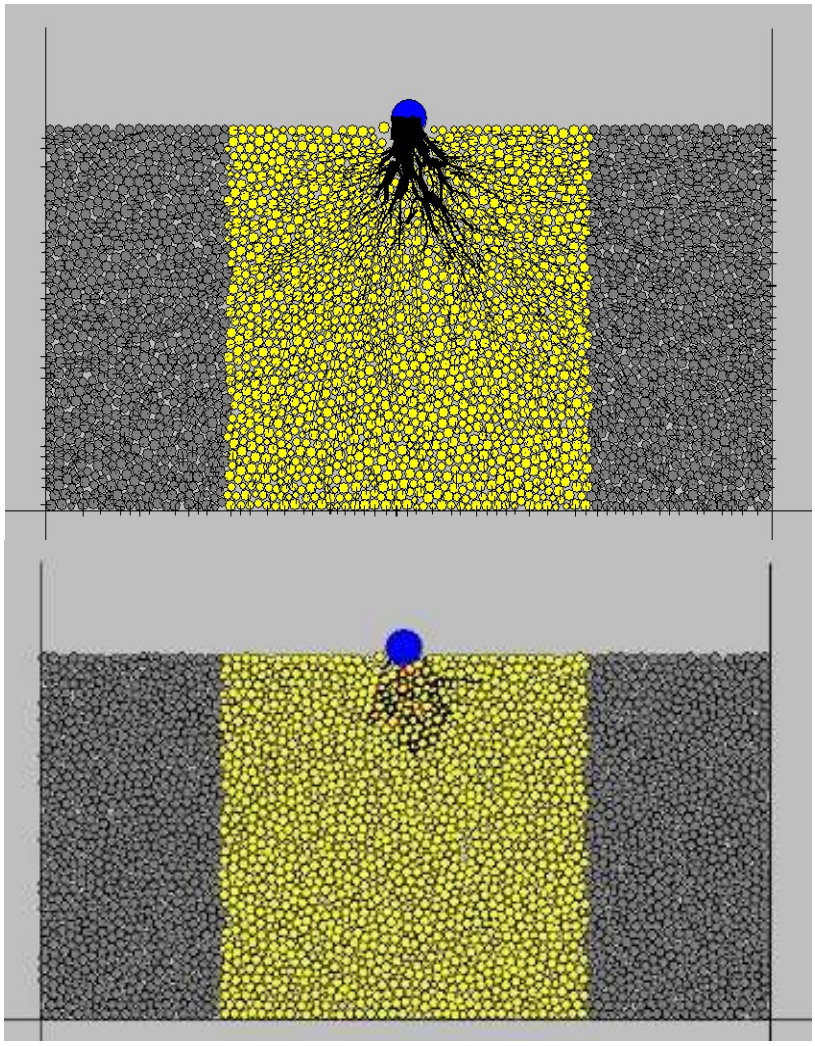

Figure 4-13: PFC2D indentation test simulation visualization result on RLM.

In Figures 4-14 and 4-15, we can find that the simulation result of the PFC2D simulation gives a similar slope (Load/ Displacement) as the first linear region of the experiment result. The IHI value (the slope of the load/ displacement curve) calculated from the PFC simulation result is 41.21 kN/mm for granite and 18.80 kN/mm for RLM. This indicates that the stress/ strain behavior of the rock in the indentation test is similar for experiment and simulation. For both rock materials, the PFC result has a similar pattern. It is observed that there are two failures are captured in the PFC2D simulation, with one

slight failure and one major failure. The simulation peak value of the load/displacement curve is similar to the experiment, while the displacement at the failure is smaller than the experiment.

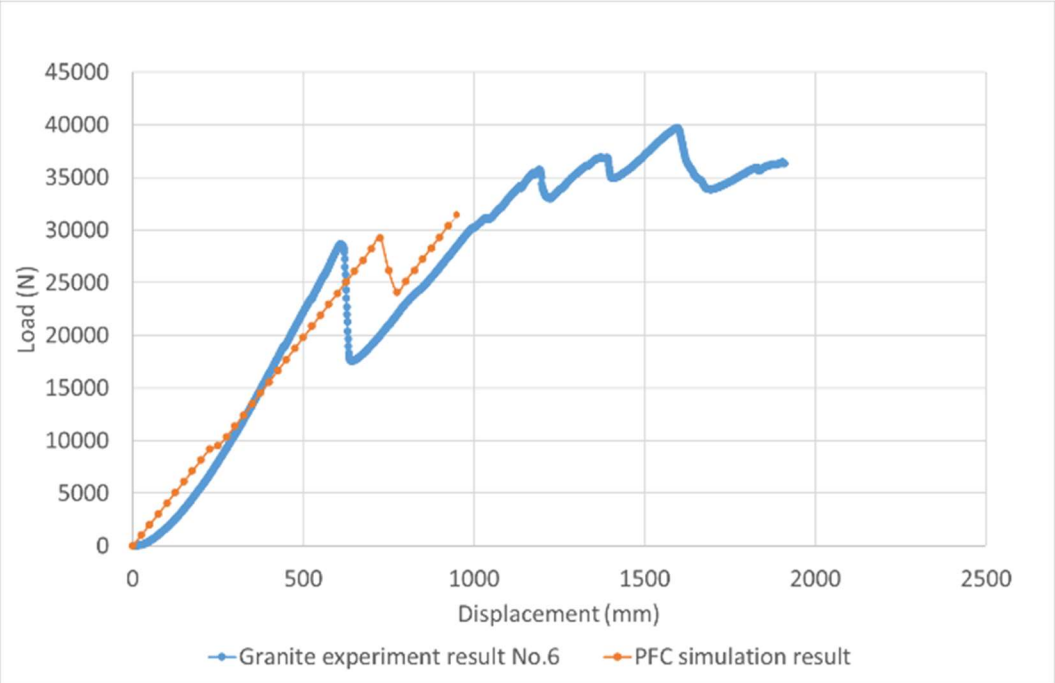

Figure 4-14: Comparison between granite indentation test experiment result and simulation result.

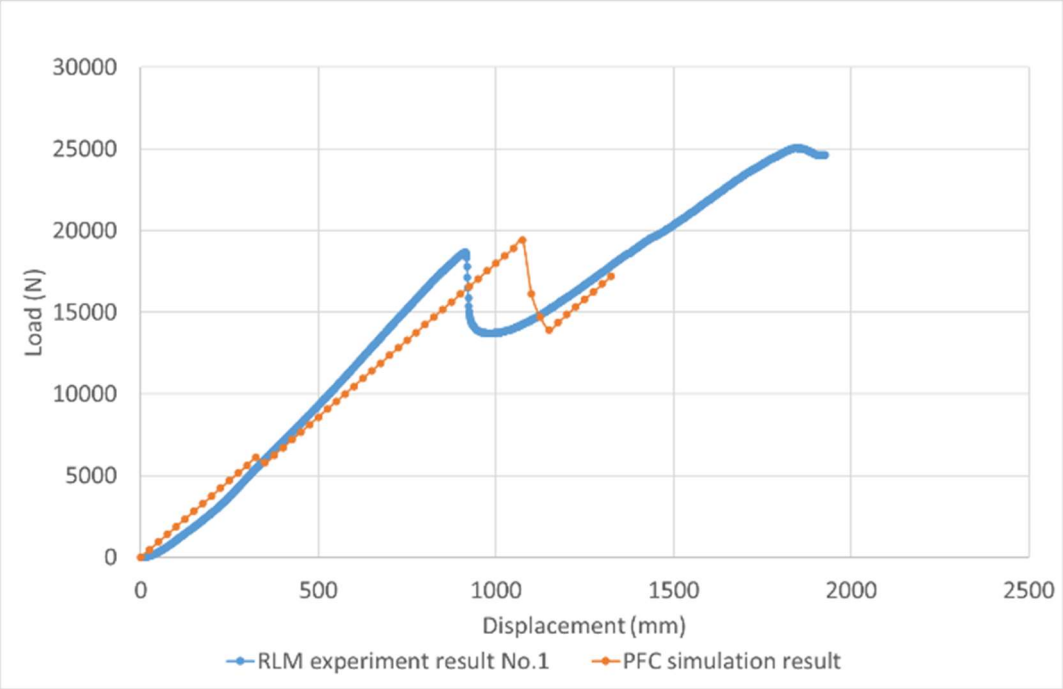

Figure 4-15: Comparison between RLM indentation test experiment result and simulation result.

4.2.5. Conclusion

Indentation tests were conducted on the granite and RLM materials and the experiment data is analyzed. It is observed that the RLM UCS calculated from the slope (Load/Displacement) agrees well with the UCS experiment result, according to the previous empirical correlation. The granite, however, requires a minor correction on the coefficient used in the correlation.

The simulation result of the granite and RLM are compared with the experiment result. The simulation result slope is nearly constant and the non-linear region is not observed as in the experiment result. The reason could be that the ductile property of the material is not completely characterized in the simulation model. The slopes of the simulation result turn out to be slightly lower than the experimental result. It is assumed that the

fact that mechanical properties assignment on the surrounding wall does not exactly match the metal strap used in the experiment could explain this difference. The peak load also shows a difference between the experiment result and the simulation result, however, it does not influence the calculation of IHI and thus UCS.

In the future, more indentation tests will be conducted on high-strength RLM and granite. The PFC2D DEM model will be optimized to better represent the rock failure property during the indentation test.

Chapter 5. Evaluation of Indentation on High Strength and Isotropic Formations

5.1 Introduction

Mining and Oil and gas industry spends a lot of money on excavation technology (Denkena, 2022). The efficiency of the tool is meant to increase by excavating a unit volume of rock by applying minimum energy. The tool geometry is thus a deciding factor to enhance the drilling efficiency. The mechanism by which the drilling bits used in oil and gas drilling and disc cutters in mining break rock is called indentation (Copur, 2003). Laboratory indentation on rocks give us the similar responses as the tools used in field for large scale excavation purposes. A metallic indenter that is used to replicate the bit teeth is forced against a rock specimen and the loading curve is utilized for further rock breakage investigation. In this indentation process, variables such as size of the rock sample, confinement around the sample, indenter geometry have certain effects on the loading curve and the rock breakage. In this study a servo controlled loading frame is utilized in providing a constant loading rate to the indenters forcing against rock cores. The specimen used in this study is granite which is a hard and isotropic rock. Core specimens in different sizes are subjected to varying confinements around their circumference using metallic straps. Also, metallic indenters with varying tip diameters were tested in combinations with rock samples with varying sizes and confinements. The purpose of this study was to study the effect of individual variable on the loading curve of indentation test. Indentation also ends with a crater formation in the rock. The

volume of the craters were utilized in specific energy study based on the work done in crater formation.

Similar to the work done in chapter 4, this research was completed through team effort. Dr. Stephen Butt supervised the experimental work and made significant contributions in editing the final draft of the manuscript. Dr. Abdelsalam Abugharara coordinated with the technical services at MUN Engineering to see the manufacturing of the apparatus for the experiment to completion. Zijian Li assisted in performing the experiments and processing the data. Prajit Premraj proposed the plan for the work, prepared the samples, performed the tests, analyzed the data, and wrote the paper with the conclusions made from the experiments.

5.2 Evaluation of Indentation on High Strength and Isotropic Formations (Manuscript #2 from GeoCalgary 2022 conference organized by the CGS)

Prajit Premraj[1], Zijian Li[1], Abdelsalam Abugharara[1, 2], Stephen Butt[1]

[1]Faculty of Engineering and Applied Science – Memorial University of Newfoundland, St. John's, Newfoundland and Labrador, Canada

[2]Faculty of Engineering, Sebha University, Sebha, Libya

Abstract

High-performance drilling tool design requires a deep understanding of rock mechanical properties of strength and hardness. The indentation test is an indirect rock strength measurement test. Rock fracturing behaviors and responses under indentation tests represent rock hardness index that follows patterns and modes that also are produced similarly by drilling, cutting, and boring either in petroleum drilling processes or mining

operations. This work concentrates on conducting indentation tests on high-strength granite of a highly isotropic nature. Many samples of 2-inch diameter cores of different length to diameter ratios were tested using different indenter-tip diameters with varying confinements to evaluate the influence of all variables in the test on rock cuttability. The tests resulted in curves with varying load-displacement responses and specific energy.

5.2.1. Introduction

Drilling and boring involve excavation of the earth's crust which requires a lot of energy. These are processes that are time-consuming and thus an expensive part of the mining and petroleum industry. Research is implemented in these disciplines to optimize these activities in an economic and time-targeted manner. Excavation of the rocks is a subsurface activity that can be learned, planned, and performed using rock engineering principles. Before and after visualization is the only way to study rock tests due to their opaque nature (Swain, 1976). Effective tool design requires the strength of rock as a physical parameter Denkena (2022). These values are obtained by direct rock tests such as unconfined compressive strength (UCS), Brazilian tensile strength (BTS), etc. devised by the ASTM standards. Direct tests are usually expensive, time-consuming, complicated, and less adaptable to field conditions (Kallu, 2015). Also, the sample preparation must be precise, crack-free, and discontinuity free.

In conditions when the rock samples to be studied are not available in bigger sizes and sophisticated requirements so as to perform standardized tests, Szwedzicki (1998) came up with a draft to help engineers categorize rocks based on their hardness. He added some correlations to predict the unconfined compressive strength of rocks using slope from the load-displacement curve from rock indentation, also known as IHI (Indentation hardness

index) with less sophisticated sample preparation. In the next two decades, indentation tests underwent many modifications and changes. Though the process varied, the output from the tests gave similar justifications. Kalyan (2015) presented a review comprised of all the work done and advancements made in the indentation tests for rock hardness evaluation.

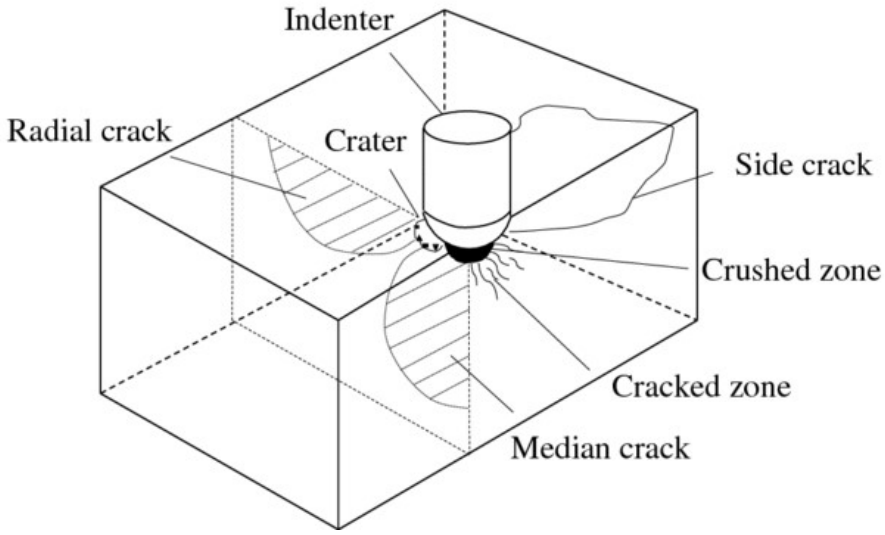

Figure 5-1: Fracture pattern occurring in rocks by indentation. (Saadati, 2018)

Ranman (1985) described the process of indentation as a cycle that can be divided into three sections. It begins with the indenter stored with elastic energy that subsequently causes crushing. The further increase in load extends the crack formation until the load drops significantly and another cycle begins. The main objectives of the indentation tests were to primarily understand rock breakage, predict the rate of penetration and optimize excavation tool development, and secondarily find rock strength.

Kaharman (2012) developed comprehensive correlations between the indentation

hardness index (IHI) with UCS and BTS including all three types of rocks occurring in nature: igneous, metamorphic, and sedimentary. This work highlighted the strong correlation between the IHI and UCS. The experimental setup and procedures are very well described and a statistical study added to the experimental work provided more confidence in the conclusions. Copur (2003) utilized indentation tests for predicting cutter performance and mechanical properties of the rocks. As the disc excavation mechanism matches the indentation process, the indentation indices are obtained for the studies from his apparatus. Mateus (2007) utilized the indentation testing technique on irregularly shaped rock specimens to predict rock parameters utilizing the Kaharman (2012) correlations. This work concluded that, since there are no adopted standards for indentation tests, different researchers often yield conflicting results due to differences in selecting test parameters. Haftani (2014) proved that the cross-sectional area perpendicular to the direction of loading does not matter as much as the thickness of the sample since results showed that greater thickness resulted in higher IHI. His experimental apparatus applied lateral confinement to the rock sample leading to higher indentation loads at crater formation and sample failure by splitting. Yin (2014) conducted disc cutter indentation experiments with confinement on granite and marble. He found that increasing the confinement increases the force required to initiate a crack and the size of the crushed zone, and as confinement around the rock surface increases, there is a transition from brittle to ductile fracturing.

Hood (1977) concluded that cone indenters require more penetrating force than wedge indenters to break through the rock, but an added shear or transverse force reduces the penetrating force, making cutting easier and more efficient. This principle is used in

designing tools that utilize roller cones and disc cutters. Benjumea (1969) studied the responses of indentation on non-isotropic rocks by keeping the indenter geometry the same. He also carried out experiments on rock breakage parameters based on penetrating through the bedding of the rock with an indenter in directions perpendicular and parallel to the bedding. The work also discussed a technique to calculate specific energy utilized in the indentation process by measuring the crater volume by filling it with a displacing fluid from a burette. Zou et al. (2022) measured specific energy using a laser crater profiling method and observed that increasing confining pressure around the sample increased the specific energy for crater formation. Zhu (2020) carried out a comprehensive study on the crack formation and propagation in rocks under an indentation test, finding a total of 4 types of cracks in rocks, namely: Intra grain shear, intra grain tensile, inter grain tensile, and inter grain shear Out of all of these types, the most prevalent type of crack observed during indentation is the inter grain tensile crack. The mechanism of crack formation will vary based on rock structure and grain size distributed inside the bulk of the rock.

In this paper, granite core samples of 2-inch diameter with varying length to diameter ratios are used in the indentation test. Various combinations of the metal indenters' spherical tip diameter and the confinement pressure around the rock side surface are included in the test sample matrix. The test is performed utilizing a servo-controlled frame with a constant loading rate. The rock cuttability is discussed based on the slopes of the curve, the load levels at which the samples break, and the specific energy spent in breaking them.

5.2.2. Materials And Methods

5.2.2.1 Servo Controlled Loading Frame

Memorial University Materials Lab's servo control frame has a maximum load capacity of 250kN. It can conduct compressive and tensile strength tests at specified custom loading rates, which may be regulated by either displacement or load control. The displacement control loading is used in this work to avoid quick indentation, which causes a substantial fracture propagation in the rock sample. A loading rate of 0.01mm/sec was selected based on the previous experimental procedures devised by various researchers including Copur (2003) and Haftani (2014, 2015).

Figure 5-2: Servo controlled loading frame.

5.2.2.2 Metallic Indenters for the Test

Figure 5-3: Metallic indenters with varying tip diameters. From left to right 7 mm, 5 mm, and 3 mm.

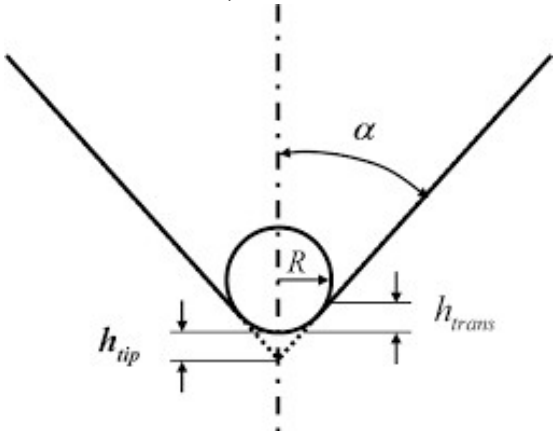

Figure 5-4: Geometry of a conical metallic indenter. (Szwedzicki,1998).

In figure 5-4, angle α is called the apex angle which is set at a constant value of 60° for all the indenters in this study. R is the radius of the spherical tip of the indenter. All the indenters are made from hardened steel with a hardness of 58 HRC. The tips of the indenters are spherical. The test utilizes 3 geometries with tip diameters of the sphere as 7 mm, 5 mm, and 3 mm.

5.2.2.3 Rock samples and confinement setup

Granite core samples were utilized after being cored from blocks of the rock using a 2-inch coring bit. The long core samples were later cut into disk samples with heights of 1 inch and 2 inches respectively. The intention of this was to prepare samples with dimensional criteria with a length to diameter ratio of 0.5 and 1. Both types of rock samples are saw-cut and are ensured to have a smooth and flat surface. This is done to the samples to ensure they yield accurate results. Two metal straps of different heights were manufactured to cover the circumference of each of the samples. The strap was tightened by nut and bolt to offer selected confinement values while testing using a torque wrench.

Figure 5-5: Granite core samples and confining metal straps for the experiment.

5.2.3. Experimental Procedure

The prepared granite core samples are placed on a core platen on the servo-control loading frame and the indenter is lowered until the tip of the indenter contacts the smooth

rock surface with a minimum load of 12 Newton force. This ensures that the rock is engaged and the testing can proceed. A constant loading rate of 0.01mm/sec was applied to the indenter at the beginning of the test. The test continued for 3 minutes which accounts for a 1.8mm displacement. All the tests split before 3 minutes, but the same procedure was repeated for all the samples. The servo control loading frame produced a real-time load-displacement plot while the experiments were performed. There were 15 tests done on the smaller 1-inch long samples and 32 tests on the bigger 2-inch long samples, with and without the metal strap confinements.

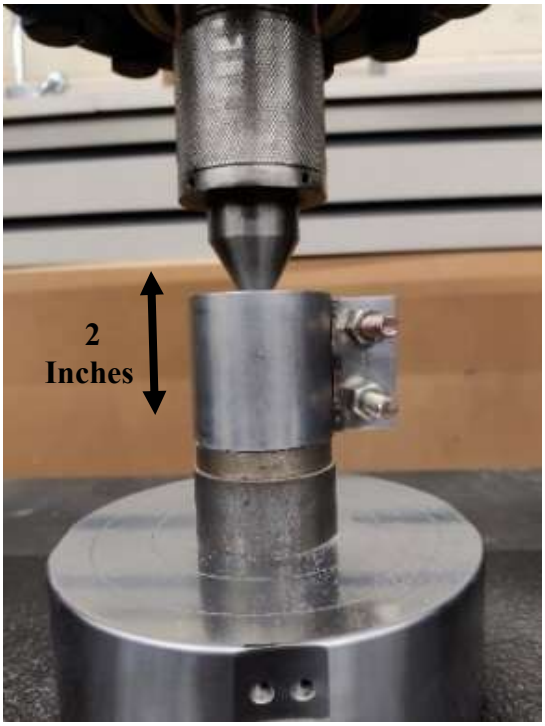

Figure 5-6: Sample with length to diameter ratio of 0.5 undergoing indentation subjected to confinement using a metal strap.

A torque wrench is utilized to tighten the metal straps to the required torque on the nut-bolt assembly. The torque values used in this experimental work are 0 Nm, 7.35 Nm, and 8.48 Nm respectively.

We use specific energy as a parameter to evaluate the rock penetration efficiency. The specific energy is affected by the variation of other parameters, such as indenter tip diameter and confinement around the rock. Specific energy in this work (Joules) is calculated by dividing the work done in breaking the rock under the load-displacement curve by the volume of the spherical tip of the indenter which is displaced into the surface while loading.

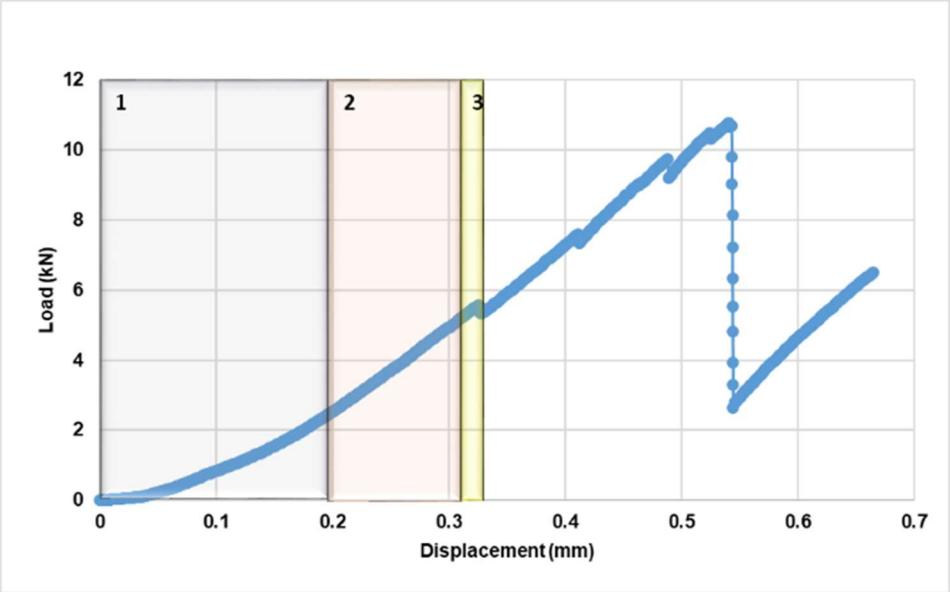

Figure 5-7: Indentation curve highlighting zone transition with loading.

In Figure 5-7, the plot achieved from the loading of the granite rock is highlighted in 3 different zones. Zone 1 denotes the section where rocks behave elastically. Zone 2 highlights the part where that elastic nature turns into plastic and the slope starts to become more linear; this is the zone of interest from which the indentation index is calculated. Zone 3 is the neck of the curve where the rock no longer is crushed and a crater is produced along with a drop in the load.

5.2.4. Results And Discussions

A total of 47 tests were performed. From Figure 5-8, the six samples to the left had been indented with no confinement, and the nine to the right were confined with a torque value at the nut and bolt at 8.48 Nm.

Figure 5-8: All samples with L: D of 0.5 post indentation.

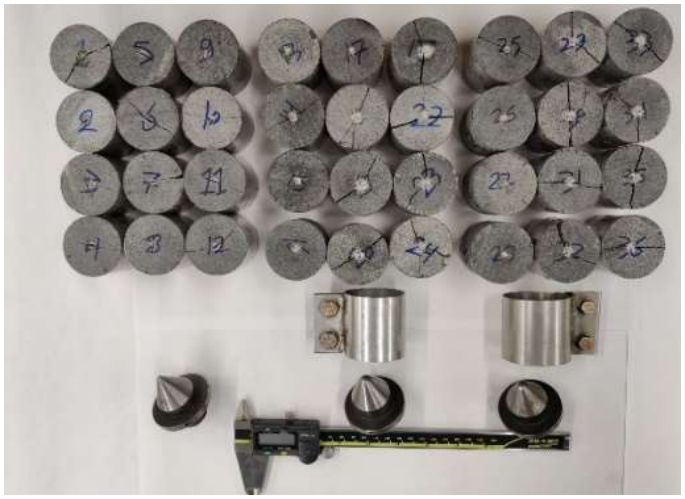

Figure 5-9: All samples with L: D of 1 post indentation.

In Figure 5-9, the samples are arranged in such a way that there are 3 sets of 3 columns. The samples are arranged into 3 sets to represent the confinement the samples were subjected to. As the first one does not have the metal strap below, it says 0 Nm confinement. The second and third are 7.35 Nm and 8.48 Nm respectively. The 3 columns represent the different indenter tips used for testing in the order of increasing tip diameter from 3 mm to 7 mm respectively.

The indentation test gives a result of the load-displacement response for a certain rock type, which is influenced by other variables involved in the test. These variables can be loading rate, rock type, rock mineralogy composition, indenter geometry, and sample confinement. In this work, the rock sample is obtained from granite, which is a typical isotropic rock. The indenters tip diameter and confinement around the samples are varied and their influence on the indentation test result is then analyzed.

5.2.4.1. Effect of Indenter tip diameter and Confinement around the core sample

As we go from a smaller tip diameter to a higher tip diameter, experimentally, the cratering of rock becomes difficult. This means that more load is required in breaking the rock. This is analytically observed from the rock's loading curve. The flatter the curve, the easier it is to break it, and the farther it goes away from the horizontal axis, the more the difficulty to break the rock increases. The slope is calculated from the transition of elastic to the plastic zone where the curve is linear and straight and is called the indentation hardness index. In Figure 5-10, all the rock samples are subjected to no confinement around them. A significant difference in slope is noted when the 3 mm tip diameter of the indenter is used. The curve is very flat but as we move to a 5 mm tip

diameter, the value of the slope of the curve and the indentation index jump up by 2.5 times. The slope of the 7 mm tip is 10% more than the 5 mm tip diameter results. It is seen that with increasing tip diameter, the angle of slope keeps increasing. The slopes from 5 mm and 7 mm tip diameter are very close to each other, but the 3 mm diameter tip breaks the rock easily with a much narrower tip. A total of 4 experimental slopes were averaged for the analysis for Figure 5-10 on samples with a length to diameter ratio of 1.

The tightening from the torque wrench provided more confinement to the rocks laterally. Any solid body when subjected to vertical stress tries to compensate laterally. Rocks do have an elastic nature in their early indentation zone. Confinement around the rock prevents that action. According to Mohr's circle, a confined body of uniform composition has a delayed fracture that fails the rock rather than a rock with no confinement (Rajagopal, 1998). For understanding, samples with a length to diameter ratio of 1 were subjected to different confinement levels and indented using a 7 mm tip diameter indenter. The results are expressed in Figure 5-11.

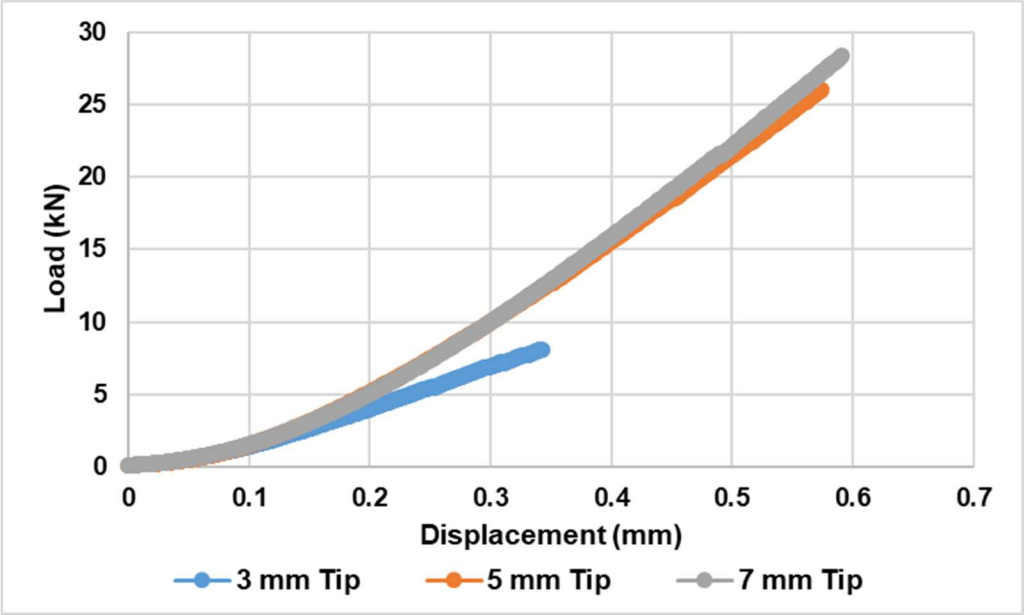

Figure 5-10: Indentation test slope response for different indenter tip diameters without any confinement.

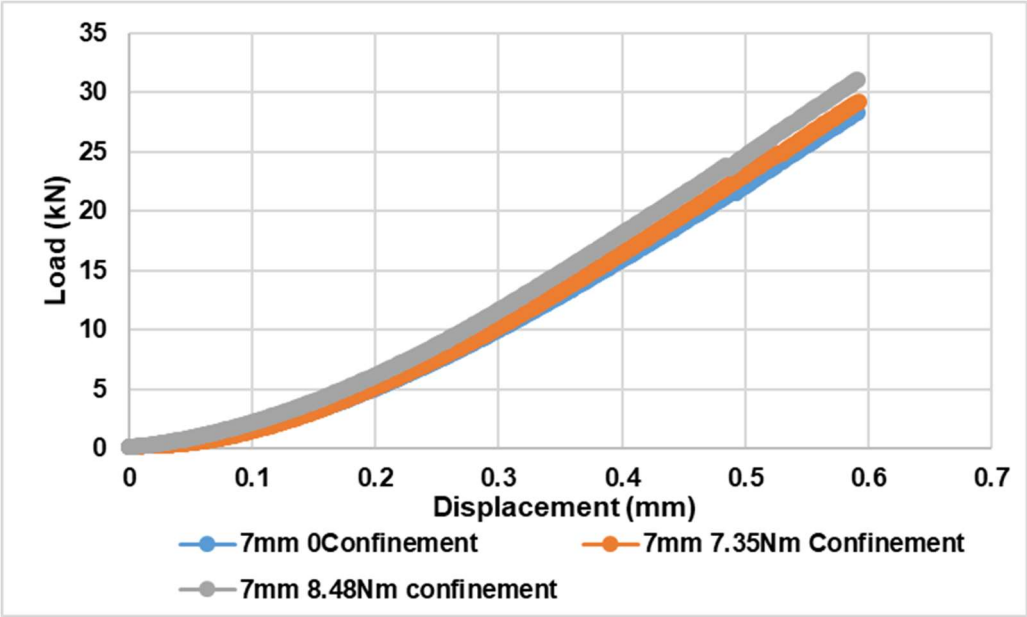

Figure 5-11: Indentation curve for 7mm indenter tip diameter with varying confinements for samples with L: D of 1.

Another fact noticed is that the point at which the rock fails and splits is shifted ahead. In Figure 5-11, we can notice the slopes - depicted by different colors - are not only shifted positively on the vertical axis but are also shifted positively on the horizontal axis. A similar pattern is observed with increasing the confinement around the core sample (Premraj, 2022)

Table 5-1: Results of indentation tests for samples with L: D of 0.5.

Tip Diameter	Confinement	Average slope	Std dev
mm	Nm	kN/mm	kN/mm
3	0	25.01	2.91
5	0	51.35	2.20
7	0	59.05	3.67
3	8.48	27.12	0.24
5	8.48	54.54	2.52
7	8.48	65.48	0.07

Tables 5-1 and 5-2 above numerically present the results from the tests with a very small standard deviation. This proves that the tests were very consistent and repeated with an average standard deviation of 1.194kN/mm. The peak value of indentation is the value at which the rock splits when subjected to a certain amount of load corresponding to the displacement of the indenter into the rock surface. The peak value achieved at a 5 mm tip is twice the peak value at a 3 mm tip diameter, whereas with a 7 mm tip, the value is

2.4 times that achieved from a 3 mm tip diameter. This means the results from 5 mm and 7 mm are very similar and also very different from 3 mm tip diameter.

Table 5-2: Results of indentation test for samples with L: D of 1.

Tip Diameter	Confinement	Average slope	Std dev
mm	Nm	kN/mm	kN/mm
3	0	22.91	1.63
5	0	56.62	2.40
7	0	63.99	2.66
3	7.35	25.22	3.02
5	7.35	56.96	1.41
7	7.35	59.75	1.21
3	8.48	27.69	2.17
5	8.48	58.28	0.75
7	8.48	65.83	1.87

The failure index is the peak value with a load and corresponding displacement value at which the rock fails and splits in half. This index denotes failure of rock and helps to correlate failure with parameters of indentation such as slope.

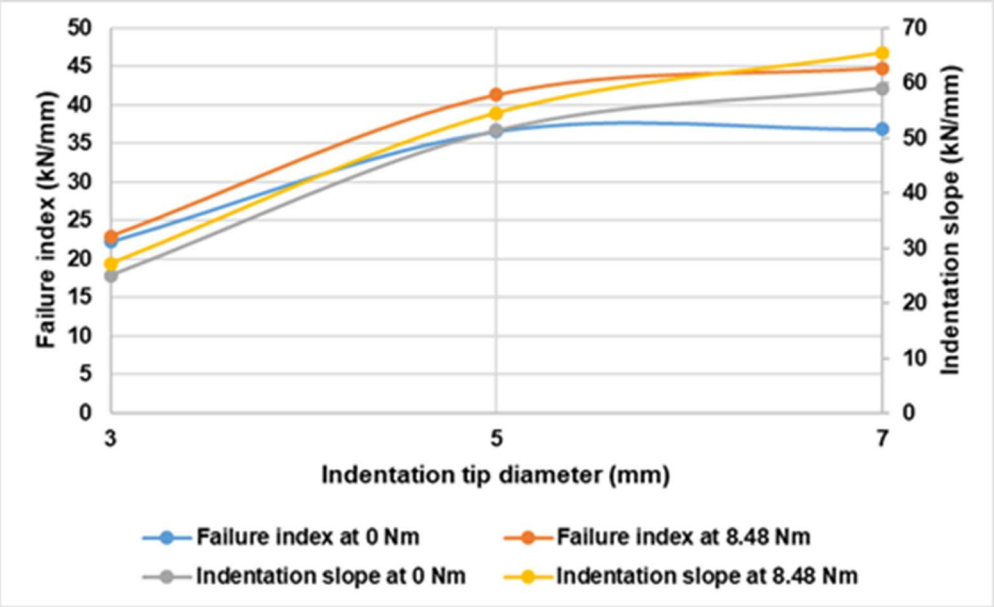

Figure 5-12: Influence of confinement and indenter tip diameter on indentation indices for L: D of 0.5.

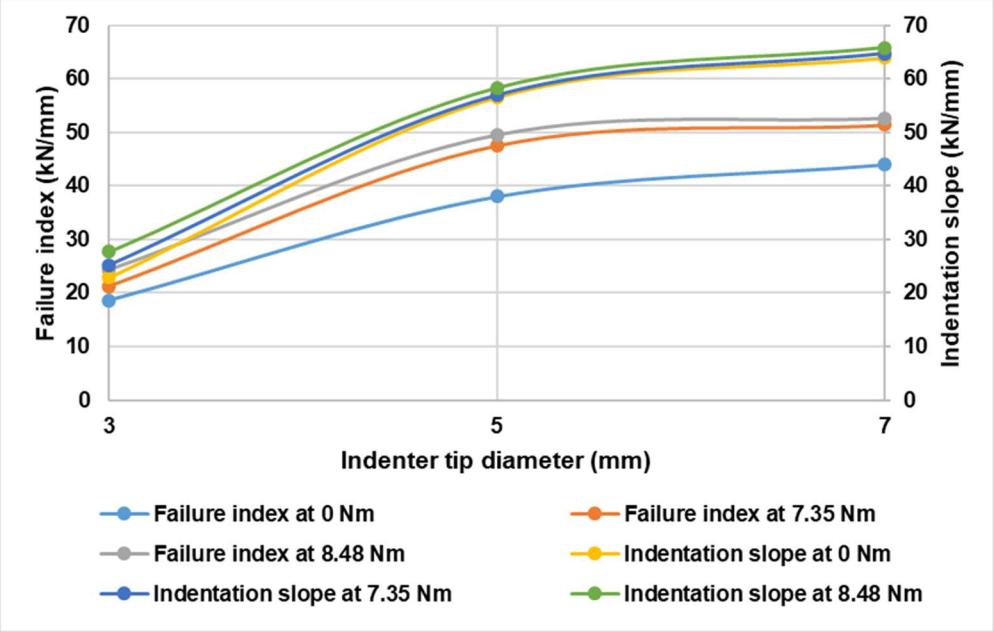

Figure 5-13: Influence of confinement and indenter tip diameter on indentation indices for L: D of 1.

In these two graphs from Figure 5-12 and 5-13, the variation in tip diameter of the indenter and the confinement around the rock are correlated with the slope of the indentation curve as well as the failure index. The shift is consistent and is in the positive axis with increasing tip diameter and confinement.

5.2.4.2. Effect of size of the rock core sample

The size of the sample influences the outputs of the indentation tests (Haftani, 2014). Smaller samples with a length to diameter ratio of 0.5 break earlier and easier than samples with a length to the diameter of 1. As the height of the sample increases, the extension of the median crack that breaks the rock is delayed. This is graphically evident. Because of the ease with which the smaller samples break, their slopes and peak index are 10% smaller than the larger samples. Median cracks, as shown in Figure 1, are the type of cracks that travel to the base of the sample from the bottom of the tip indenter when loading occurs. Shetty (1985) concluded in his work that the length of the median crack is linearly proportional to the Indentation load. This means it requires more load to produce a long median crack. From the experiments, we found out that the samples with a length to diameter ratio of 1 failed under loads higher than the samples with a length to the diameter of 0.5. This is experimentally verified in this study. There is an interesting observation made from the test using confinement at a torque value of 8.48 Nm around both the core samples with different heights. The slopes using this confinement give a similar value and, as a result, from Figure 5-14 we can see the slopes of the two types of samples overlapping each other. In this condition, the effect of the size of the sample is eliminated as the slope is the parameter that is most useful to us.

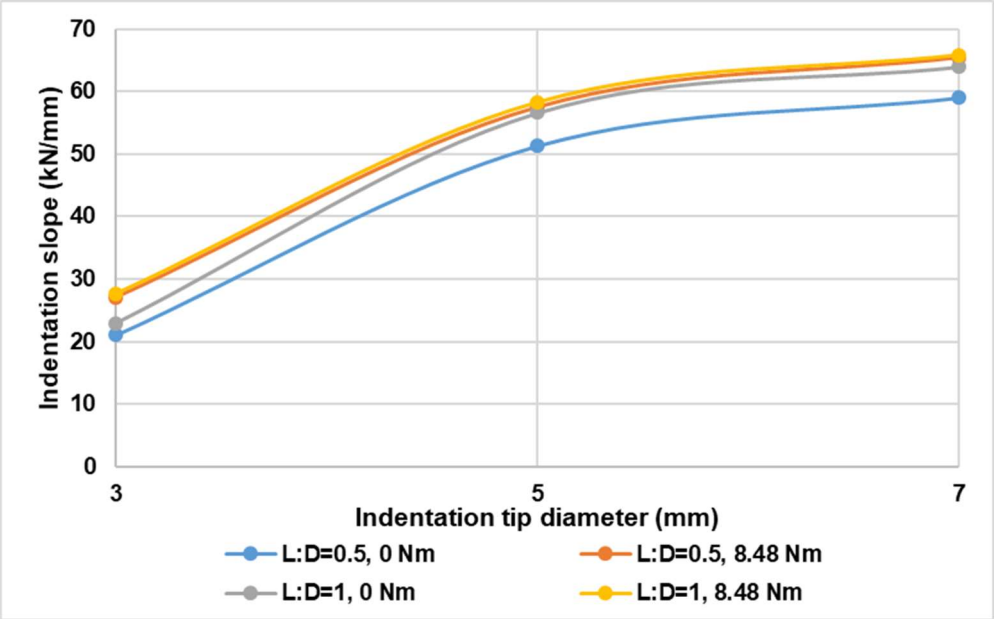

Figure 5-14: Effect of confinement on size of the sample.

5.2.4.3. Effect of Specific Energy

Specific energy is the work done to excavate a unit mass of rock by the tool. This study helps understand a pattern of how the specific energy varies with confinement around the core sample and the varying tip diameter of the indenter. The higher the confinement around the rock, the more energy that has to be spent to excavate a unit volume. This means that specific energy at no confinement is lesser than that at confinement from a torque value of 8.48 Nm.

On the other hand, as we move from a smaller tip diameter to a higher tip diameter, the specific energy drops down. This is because a bigger tip diameter corresponds to more volume of the metallic indenter displaced into the rock surface at the same displacement value. Ma (2016) drew conclusions from his work on confining granite for tunnel boring

machine performance. TBM primarily breaks the rock by indentation or forces normal to the rock surface. He found out that with increasing penetration, the specific energy values decreased for a very long range. In this experimental work moving from smaller to higher tip diameter, the penetration has constantly increased while the specific energy has decreased. Also, with increased confinement, the specific energy utilized for rock breakage keeps rising. Zou (2020) experimentally and numerically proved that specific energy is negatively correlated to the indentation hardness index.

Experiments conducted by Zhang (2021) on limestone had the same pattern where the specific energy invested was more on confined samples than the unconfined samples.

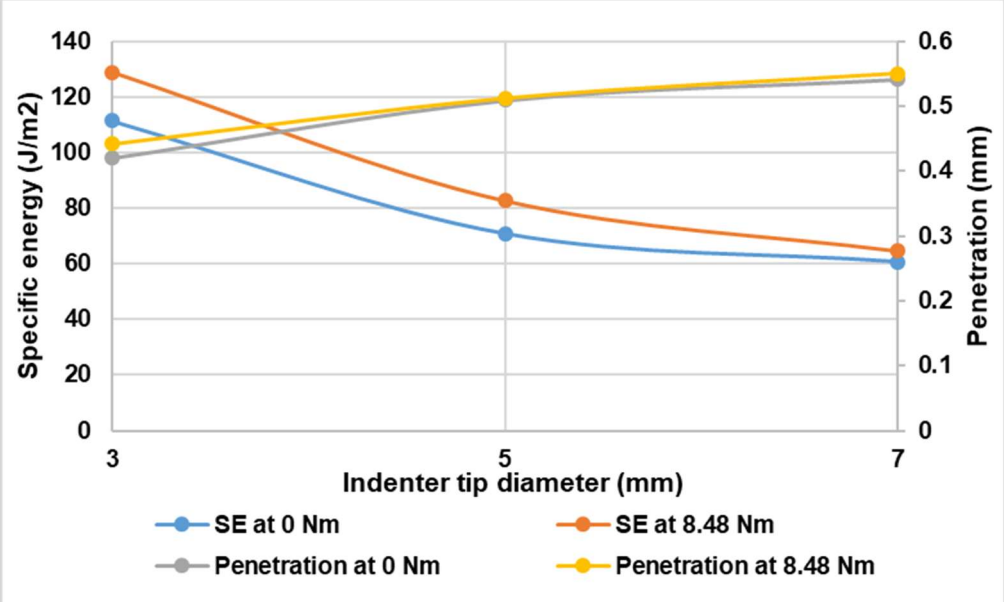

Figure 5-15: Effect of indenter tip on specific energy and penetration for samples with L: D=0.5.

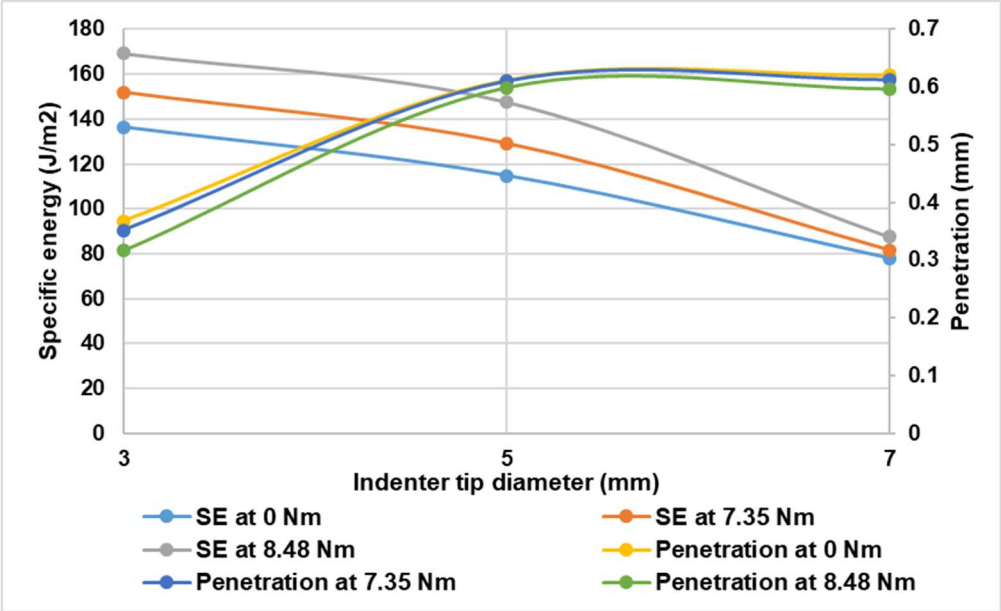

Figure 5-16: Effect of indenter tip on specific energy and penetration for samples with L: D=1.

Table 5-3: Specific energy analysis from indentation.

Torque	Tip diameter	Height indented	Indented volume	Work	Specific Energy
Nm	mm	mm	mm3	Joules	Joule/m2
0.00	3.00	0.368	10.35	1411.4	136.40
7.35	3.00	0.352	9.91	1504.2	151.82
8.48	3.00	0.416	11.69	1977.9	169.22
0.00	5.00	0.611	47.75	6962.7	145.81
7.35	5.00	0.610	47.68	7348.8	154.14
8.48	5.00	0.599	46.84	6917.0	147.68
0.00	7.00	0.620	95.18	7417.7	77.94
7.35	7.00	0.613	94.08	7402.7	78.69
8.48	7.00	0.597	91.69	7663.0	83.58

5.2.5.Conclusions

The effect of varying indenter tip diameter, confinement around the sample, and the height of the samples were studied on granite. The major conclusions drawn from the work are:

- With increasing tip diameter, the angle of the slope keeps increasing hence the load required to indent into the rock by unit distance increases.
- The slope of the indentation curve jumps up to almost twice the value as we transition from 3 mm to 5 mm and 7 mm tip diameters.

- The confinement hinders the rock breakage and delays the fracture. This is because the lateral expansion while a crater is generated is obstructed by stiff walls, hence the median crack does not propagate to the bottom to break the rock. Therefore, the difficulty in penetrating through a confined rock increases the rock indices.
- Increase in the size of the sample works the same way. The crack requires more load to travel to the other end of the rock sample to break it, therefore the slope and the failure are shifted ahead while moving from a shorter sample to a taller sample.
- There is an interesting fact found that the slopes of the curves of indentation overlap for the smaller and the bigger samples when both were subjected to confinement at 8.48 Nm torque around the core. This eliminated the size dependency.
- With increasing tip diameter, the specific energy utilized to break the rock kept decreasing. On the other hand, for the same indenter type, the specific energy increased with increased confinement.
- With the increasing penetration of the indenter, the specific energy kept dropping down consistently.

Chapter 6. Conclusions and Recommendations

After introducing and expressing the objective of this thesis along with a comprehensive literature review, a dedicated chapter enumerates the experimental procedures. This Chapter, Chapter 3, deals with individual apparatus utilized for study. A sophisticated sample preparation procedure is then described for the two different studies in Chapters 4 and 5 respectively. Following this, a stepwise procedure for performing the test and finding various parameters is well described. Lastly, for the evaluation of hardness of isotropic rocks, indentation tests were performed on granite and synthetic rocks.

For the first study, the sample preparation methods were replicated from preliminary work done in past research for this type of testing. These experiments were initially performed in the laboratory. Based on the parameters used in the experiment, the exact same model was recreated successfully using a DEM (Distinct Element Modelling) method by the PFC2D package. The graphical results of loading during the indentation tests in the numerical model were found to be very close to the experimental results. The slopes from the linear section of the loading curve from the test were utilized in successfully predicting the strength of the rock type with minor adjustments to the indentation coefficients. The loading curve generated by the numerical model was only marginally different from the experimentally derived loading curve. The absence of the elastic zone in the initial phase of the indentation in the DEM model is due to the inability to characterize the ductile property of the rock. In addition, the conversion of the torque on the metal strap to a corresponding pressure value would assist the simulation results to be consistent with the experimental results. More work in tackling these two challenges needs future study.

The second study dealt with the same type of experiment but with less sophisticated sample preparation compared to the previous chapter. This was a comprehensive study conducted to find responses to rock indentation by changing variables in the test. More specifically, these variables included the geometry of the indenter, the size of the rock core specimen, and the confinement around the rock. As we go from smaller to larger tip diameter for the metallic indenter, the load required to form a crater on the rock core increases; this is represented by a flatter to narrower transition in the loading slope of the curve. The confinement around the rock contributes to a similar pattern in the loading curve.

Moving from zero confinement to maximum confinement, the force required to create a crater significantly increases. The size of the core samples can also contribute to varying indices. More specifically, size is classified by a length-to-diameter ratio. A sample with a lesser length-to-diameter ratio was termed as a smaller sample compared to one with a higher length-to-diameter ratio. The difficulty in propagating the median crack from the top of the rock to the bottom increases with an increase in height of the rock core, so failure in the taller samples occurs at a load value much higher than in a shorter sample of the same rock type. There was an interesting result when the smaller and the larger samples were subjected to maximum confinement; it was found that the slope from the loading curve was similar at maximum confinement for both sizes of the rock samples.

A method was devised to find the volume excavated in cratering the rock with changing indenter geometry. This helped us find the Specific Energy spent in that process. From the analysis conducted, it was found that the specific energy in forming a crater was directly proportional to the confinement around the rock sample and inversely proportional to the tip diameters of the indenter. This pattern was seen to repeat itself for both sizes of the

rock samples. Lastly, with increasing penetration, a decrease in the Specific Energy was observed.

References

Benjumea, R., & Sikarskie, D. L. (1969, July). A note on the penetration of a rigid wedge into a nonisotropic brittle material. In *International Journal of Rock Mechanics and Mining Sciences & Geomechanics Abstracts* (Vol. 6, No. 4, pp. 343-352). Pergamon.

Bilgin, N., & Kahraman, S. (2003, June). Drillability prediction in rotary blast hole drilling. In *Proc. 18th Int. Mining Congress and Exhibition of Turkey, Antalya, Turkey* (pp. 177-182).

Carpinteri, Alberto, and Stefano Invernizzi. "Numerical analysis of the cutting interaction between indenters acting on disordered materials." *International journal of fracture* 131, no. 2 (2005): 143-154.

Copur, H., Bilgin, N., Tuncdemir, H. & Balci, C. "A set of indices based on indentation tests for assessment of rock cutting performance and rock properties." *Journal of the Southern African Institute of Mining and Metallurgy* 103, no. 9 (2003): 589-599.

Denkena, B., Breidenstein, B., Krödel, A., Bergmann, B., Picker, T., & Wolters, P. (2022). Suitability of natural rocks as materials for cutting tools. *SN Applied Sciences*, *4*(1), 1-21.

Dong, G., & Chen, P. (2017). A comparative experimental study of shale indentation fragmentation mechanism at the macroscale and mesoscale. *Advances in Mechanical Engineering*, *9*(8), 1687814017726244.

Entacher, Martin, Stefan Lorenz, and Robert Galler. "Tunnel boring machine performance prediction with scaled rock cutting tests." *International Journal of Rock Mechanics and Mining Sciences* 70 (2014): 450-459.

Fernando, P. K. S., Pei, Z. J., & Zhang, M. (2020). Mechanistic cutting force model for rotary ultrasonic machining of rocks. *The International Journal of Advanced Manufacturing Technology*, *109*(1), 109-128.

Haftani, M., Bohloli, B., Nouri, A., Javan, M. R. M., & Moosavi,M. (2014). Size effect in strength assessment by indentation testing on rock fragments. *International Journal of Rock Mechanics and Mining Sciences*, *65*, 141-148.

Haftani, M., Bohloli, B., Nouri, A., Javan, M. R. M., Moosavi, M., & Moradi, M. (2015). Influence of penetration rate and indenter diameter in strength measurement by indentation testing on small rock specimens. *Rock Mechanics and Rock Engineering*, *48*(2), 527-534.

Haftani, Mohammad, Bahman Bohloli, Mahdi Moosavi, Alireza Nouri, Majid Moradi, and Mohammad Reza Maleki Javan. "A new method for correlating rock strength to indentation tests." *Journal of Petroleum Science and Engineering* 112 (2013): 24-31.

Hood, M. (1977). Phenomena relating to the failure of hard rock adjacent to an indentor. *Journal of the Southern African Institute of Mining and Metallurgy*, *78*(5), 113-123.

Huang, H., B. Damjanac, and E. Detournay. "Normal wedge indentation in rocks with lateral confinement." *Rock Mechanics and Rock Engineering* 31, no. 2 (1998): 81-94.

In *International Journal of Rock Mechanics and Mining Sciences & Geomechanics Abstracts*, vol. 13, no. 11, pp. 311-319. Pergamum, 1976.

Kahraman, S., Balcı, C., Yazıcı, S., & Bilgin, N. (2000). Prediction of the penetration rate of rotary blast hole drills using a new drillability index. *International Journal of Rock Mechanics and Mining Sciences*, *37*(5), 729-743.

Kahraman, S., Fener, M., & Kozman, E. (2012). Predicting the compressive and tensile strength of rocks from indentation hardness index. *Journal of the Southern African Institute of Mining and Metallurgy*, *112*(5), 331-339.

Kallu, R., & Roghanchi, P. (2015). Correlations between direct and indirect strength test methods. *International Journal of Mining Science and Technology*, *25*(3), 355-360.

Kalyan, B., Murthy, C. S., & Choudhary, R. P. (2015). Rock indentation indices as criteria in rock excavation technology–A critical review. *Procedia Earth and Planetary Science*, *11*, 149-158.

Leite, M. H., & Ferland, F. (2001). Determination of unconfined compressive strength and Young's modulus of porous materials by indentation tests. *Engineering geology*, *59*(3-4), 267-280.

Liggett, W. S., Low, S. R., Pitchure, D. J., & Song, J. (2000). Capability in Rockwell C scale hardness. *Journal of Research of the National Institute of Standards and Technology*, *105*(4), 511.

Liu, Mao, Jhe-yu Lin, Cheng Lu, Kiet Anh Tieu, Kun Zhou, and Toshihiko Koseki. "Progress in indentation study of materials via both experimental and numerical methods." *Crystals* 7, no. 10 (2017): 258.

Ma, H., Gong, Q., Wang, J., Yin, L., & Zhao, X. (2016). Study on the influence of confining stress on TBM performance in granite rock by linear cutting test. *Tunnelling and underground space technology*, *57*, 145-150.

Mateus, J., Saavedra, N., Carrillo, Z. C., & Mateus, D. (2007). Correlation development between indentation parameters and unaxial compressive strength for Colombian sandstones. *CT&F-Ciencia, Tecnología y Futuro*, *3*(3), 125-136.

Maurer, W. C. "The perfect-cleaning theory of rotary drilling." *Journal of Petroleum Technology* 14, no. 11 (1962): 1270-1274.

Morris, R. I. (1969, January). Rock drillability related to a roller cone bit. In *Drilling and Rock Mechanics Symposium*. OnePetro

Paluszny, A., R. W. Zimmerman, J. Potjewyd, and B. Jarvis. "Finite element-based numerical modeling of fracture propagation due to the plunge of a spherical indenter." In *48th US Rock Mechanics/Geomechanics Symposium*. OnePetro, 2014.

Pang, S. S., & Goldsmith, W. (1990). Investigation of crack formation during loading of brittle rock. *Rock mechanics and rock engineering*, *23*(1), 53-63.

Premraj, P., Zijian, l., Abugharara, A., & Butt, S. (2022). Indentation test implementation for rock strength correlation by experimental method and simulation using distinct element method. *ASME 41st Int. Conf. Ocean, Offshore and Arctic Engineering*, OMAE2022-79227.

Přikryl, R. "Some microstructural aspects of strength variation in rocks." *International Journal of Rock Mechanics and Mining Sciences* 38, no. 5 (2001): 671-682.

Quan, W. (April 23, 2021). *Material Characterization of Natural and Synthetic Rocks.* St.Johns, Newfoundland: Memorial University of Newfoundland.

Rajagopal, K., Krishnaswamy, N. R., & Latha, G. M. (1999). Behaviour of sand confined with single and multiple geocells. *Geotextiles and Geomembranes*, *17*(3), 171-184.

Rånman, K. E. (1985). A model describing rock cutting with conical picks. *Rock mechanics and rock engineering*, *18*(2), 131-140.

Rocha-Rangel, E. (2011). Fracture toughness determinations by means of indentation fracture. *Nanocomposites with unique properties and applications in medicine and industry*, 21-38.

Saadati, M., Forquin, P., Weddfelt, K., Larsson, P. L., & Hild, F. (2018). On the mechanical behavior of granite material with particular emphasis on the influence from pre-existing cracks and defects. *Journal of Testing and Evaluation*, *46*(1), 33-45.

Santarelli, F. J., S. Zaho, Giovanni Burrafato, Fabrizio Zausa, and Diego Giacca. "Wellbore stability analysis made easy and practical." In *IADC/SPE drilling conference*. OnePetro, 1996.

Shah, Md. "Investigation of drilling performance and penetration mechanism using passive vibration assisted rotary drilling technology." PhD diss., Memorial University of Newfoundland, 2020.

Shetty, D. K., Wright, I. G., Mincer, P. N., & Clauer, A. H. (1985). Indentation fracture of WC-Co cermets. *Journal of materials science*, *20*(5), 1873-1882.

Singh, T. N., Ashutosh Kainthola, and A. Venkatesh. "Correlation between point load index and uniaxial compressive strength for different rock types." *Rock Mechanics and Rock Engineering* 45, no. 2 (2012): 259-264.

Song, X., Aamo, O. M., Kane, P. A., & Detournay, E. (2021). Influence of weight-on-bit on percussive drilling performance. *Rock Mechanics and Rock Engineering*, *54*(7), 3491-3505.

Swain, M. V., & Lawn, B. R. (1976, November). Indentation fracture in brittle rocks and glasses. In *International Journal of Rock Mechanics and Mining Sciences & Geomechanics Abstracts* (Vol. 13, No. 11, pp. 311-319). Pergamon.

Szwedzicki, T. "Indentation hardness testing of rock." *International Journal of Rock Mechanics and Mining Sciences* 35, no. 6 (1998): 825-829.

Tan, X. C., P-A. Lindqvist, and S. Q. Kou. "Observation and simulation of rock indentation fracture." In *1st North American Rock Mechanics Symposium*. OnePetro, 1994.

Teale, Robert. "The concept of specific energy in rock drilling." In *International journal of rock mechanics and mining sciences & geomechanics abstracts*, vol. 2, no. 1, pp. 57-73. Pergamon, 1965.

Thiercelin, M., & Cook, J. (1988, June). Failure mechanisms induced by indentation of porous rocks. In *The 29th US Symposium on Rock Mechanics (USRMS)*. OnePetro.

Uboldi, V., L. Civolani, and F. Zausa. "Rock strength measurements on cuttings as input data for optimizing drill bit selection." In *SPE Annual Technical Conference and Exhibition*. One Petro, 1999.

Xu, Z. H., Wang, W. Y., Lin, P., Xiong, Y., Liu, Z. Y., & He, S. J. (2020). A parameter calibration method for PFC simulation: Development and a case study of limestone. *Geomechanics and Engineering*, *22*(1), 97-108.

Yin, L. J., Gong, Q. M., Ma, H. S., Zhao, J., & Zhao, X. B. (2014). Use of indentation tests to study the influence of confining stress on rock fragmentation by a TBM cutter. *International Journal of Rock Mechanics and Mining Sciences*, *72*, 261-276.

Zhang, Xiao-Ping, Pei-Qi Ji, Quan-sheng Liu, Qi Liu, Qi Zhang, and Zhi-Hao Peng. "Physical and numerical studies of rock fragmentation subject to wedge cutter indentation in the mixed ground." *Tunneling and Underground Space Technology* 71 (2018): 354-365.

Zhang, Z. X., & Ouchterlony, F. (2021). Energy Requirement for Rock Breakage in Laboratory Experiments and Engineering Operations: A Review. *Rock Mechanics and Rock Engineering*, 1-39.

Zhang, Z. X., & Ouchterlony, F. (2021). Energy requirement for rock breakage in laboratory experiments and engineering operations: A review. *Rock Mechanics and Rock Engineering*, 1-39.

Zhang, Zhen. "Development and characterization of synthetic rock-like materials for drilling and geomechanics experiments." PhD diss., Memorial University of Newfoundland, 2017.

Zhu, X., & Shi, C. (2020). On the failure mechanism of brittle granite in 2D rock indentation.

Zou, J., Yang, W., Zhang, T., Wang, X., & Gao, M. (2022). Experimental investigation on hard rock fragmentation of inserted tooth cutter using a newly designed indentation testing apparatus. *International Journal of Mining Science and Technology*.

Zinelis, S., Al Jabbari, Y. S., Gaintantzopoulou, M., Eliades, G., & Eliades, T. (2015). Mechanical properties of orthodontic wires derived by instrumented indentation testing (IIT) according to ISO 14577. *Progress in Orthodontics*, *16*(1), 1-6.

Appendix A: Tables of Experimental Data from Chapters 4 and 5

Table A- 1: Experimental results from Chapter 4 for granite rock indentation tests

Rock type	Sr.no	Load	Displacement	IHI	UCS at IT=1.09	UCS at IT=1.08	UCS at IT=1.07
					3.1(IHI)^1.09	3.1(IHI)^1.08	3.1(IHI)^1.07
		kN	mm	kN/mm	Mpa	Mpa	Mpa
GR	1	33.14	0.73	45.33	198.06	190.65	183.52
GR	2	30.67	0.65	46.97	205.91	198.14	190.66
GR	3	30.59	1.00	30.56	128.88	124.54	120.36
GR	4	11.73	0.42	28.20	118.06	114.18	110.43
GR	5	27.00	0.58	46.88	205.44	197.69	190.23
GR	6	27.93	0.62	45.05	196.75	189.40	182.32
			AVERAGE	40.50	175.17	168.80	162.67

Table A- 2: Experimental results from Chapter 4 for medium strength RLM rock indentation tests

Rock type	Sr.no	Load	Displacement	IHI	UCS at IT=1.09	UCS at IT=1.08	UCS at IT=1.07
					3.1(IHI)^1.09	3.1(IHI)^1.08	3.1(IHI)^1.07
		kN	mm	kN/mm	Mpa	Mpa	Mpa
MS	1	18.66	0.91	20.48	83.32	80.84	78.43
MS	2	17.57	0.89	19.78	80.24	77.88	75.59
MS	3	17.63	0.94	18.84	76.05	73.85	71.71
MS	4	20.60	0.98	21.04	85.81	83.23	80.74
MS	5	18.25	0.96	19.11	77.26	75.01	72.83
MS	6	18.62	1.01	18.44	74.29	72.16	70.08
			AVERAGE	19.61	79.48	77.15	74.89

Table A- 3: Experimental results from Chapter 5 for indentation on samples with L:D of 0.5

Sr.No	Tip Diameter	Confinement	Max Load	Max Disp	Peak Index	Average PI	Slope	Std Dev	Average Slope
#	mm	Nm	kN	mm	kN/mm	kN/mm	kN/mm	kN/mm	kN/mm
1	3	0.00	10.82	0.44	24.87	22.27	27.92	2.91	25.01
2	3	0.00	10.68	0.54	19.67		22.11		
3	5	0.00	18.70	0.49	38.56	36.59	53.56	2.21	51.35
4	5	0.00	16.96	0.49	34.63		49.15		
5	7	0.00	16.65	0.442	37.67	36.85	55.38	3.68	59.05
6	7	0.00	21.11	0.5858	36.04		62.73		
10	3	8.48	10.61	0.44	24.01	22.96	27.12	0.24	27.12
11	3	8.48	7.72	0.38	20.59		27.61		
12	3	8.48	11.15	0.46	24.28		26.63		
7	5	8.48	Invalid						
8	5	8.48	15.47	0.392	39.46	41.31	52.02	0	54.55
9	5	8.48	17.68	0.41	43.17		57.07	2.52	
13	7	8.48	21.59	0.45	47.66	44.81	67.59	1.54	65.49
14	7	8.48	16.74	0.44	38.41		64.51	0.07	
15	7	8.48	25.6710	0.5310	48.3446		64.3656	0.0000	

Table A- 4: Experimental results from Chapter 5 for indentation on samples with L:D of 1

Sr.No	Tip Diameter	Confinement	Max Load	Max Disp	Peak Index	Average PI	Slope	Std Dev	Average Slope
#	mm	Nm	kN	mm	kN/mm	kN/mm	kN/mm	kN/mm	kN/mm
1	3	0	Invalid						
2	3	0	7.54	0.28	26.47	18.67	29.08	1.63	29.92
3	3	0	8.18	0.44	18.54		28.47		
4	3	0	10.83	0.58	18.80		32.20		
5	5	0	26.31	0.65	40.22	38.07	55.89	2.41	56.62
6	5	0	25.59	0.72	35.34		52.69		
7	5	0	27.95	0.72	38.66		58.57		
8	5	0	27.67	0.60	46.12		59.34		
9	7	0	28.80	0.61	46.96	44.05	60.61	2.67	64.00
10	7	0	31.96	0.85	37.52		64.21		
11	7	0	30.84	0.66	46.67		67.14		
12	7	0	30.05	0.67	45.06		64.02		
13	3	7.35	9.19	0.51	17.85	21.22	24.78	3.02	25.23
14	3	7.35	9.99	0.42	24.03		29.12		
15	3	7.35	11.24	0.57	19.72		21.75		
16	3	7.35	8.41	0.36	23.30		25.26		

Table A- 5: Experimental results from Chapter 5 for indentation on samples with L:D of 1

Sr.No	Tip Diameter	Confinement	Max Load	Max Disp	Peak Index	Average PI	Slope	Std Dev	Average Slope
#	mm	Nm	kN	mm	kN/mm	kN/mm	kN/mm	kN/mm	kN/mm
17	5	7.35	32.11	0.71	45.47	50.59	58.53	1.41	56.97
18	5	7.35	29.96	0.58	51.47		55.71		
19	5	7.35	Invalid						
20	5	7.35	28.39	0.52	54.81		56.67		
21	7	7.35	30.36	0.61	49.63	51.44	64.47	1.21	59.75
22	7	7.35	31.22	0.60	51.95		67.42		
23	7	7.35	30.49	0.59	52.12		65.62		
24	7	7.35	30.81	0.59	52.06		41.50		
25	3	8.48	10.70	0.42	25.49	24.35	29.73	2.17	27.69
26	3	8.48	9.95	0.42	23.65		27.72		
27	3	8.48	9.52	0.42	22.62		24.46		
28	3	8.48	9.30	0.36	25.63		28.85		
29	5	8.48	30.00	0.59	50.84	49.58	58.38	0.76	58.28
30	5	8.48	26.67	0.57	46.62		56.87		
31	5	8.48	28.40	0.58	49.00		58.56		
32	5	8.48	29.82	0.58	51.86		59.31		
33	7	8.48	29.91	0.60	50.28	51.68	64.58	1.87	65.83
34	7	8.48	31.82	0.58	54.96		68.29		
35	7	8.48	30.89	0.60	51.92		64.10		
36	7	8.48	30.55	0.62	49.59		66.36		